Catch me if you can: Adaptation from standing genetic variation to a moving phenotypic optimum

Sebastian Matuszewski*§, Joachim Hermisson*†, Michael Kopp‡

February 24, 2015

---

*Mathematics and BioSciences Group, Faculty of Mathematics, University of Vienna, A-1090 Vienna, Austria

§Current address: EPFL SV IBI-SV UP JENSEN, AAB 0 43 (Bâtiment AAB), Station 15, CH-1015 Lausanne, Switzerland

†Max F. Perutz Laboratories, A-1030 Vienna, Austria

‡Aix Marseille Université, CNRS, Centrale Marseille, I2M, UMR 7373, 13453, Marseille, France

6 **Running Head:** Adaptation from standing variation

7 **Keywords:** Adaptation, Standing Genetic Variation, Natural Selection, Models/Simulations,

8 Population Genetics

9 **Corresponding author:**

10 EPFL SV IBI-SV UP JENSEN

11 AAB 0 43 (Bâtiment AAB), Station 15

12 CH-1015 Lausanne, Switzerland

13 Phone: +41 21 69 31490

14 Email: sebastian.matuszewski@epfl.ch

ABSTRACT

Adaptation lies at the heart of Darwinian evolution. Accordingly, numerous studies have tried to provide a formal framework for the description of the adaptive process. Out of these, two complementary modelling approaches have emerged: While so-called adaptive-walk models consider adaptation from the successive fixation of *de-novo* mutations only, quantitative genetic models assume that adaptation proceeds exclusively from pre-existing standing genetic variation. The latter approach, however, has focused on short-term evolution of population means and variances rather than on the statistical properties of adaptive substitutions. Our aim is to combine these two approaches by describing the ecological and genetic factors that determine the genetic basis of adaptation from standing genetic variation in terms of the effect-size distribution of individual alleles. Specifically, we consider the evolution of a quantitative trait to a gradually changing environment. By means of analytical approximations, we derive the distribution of adaptive substitutions from standing genetic variation, that is, the distribution of the phenotypic effects of those alleles from the standing variation that become fixed during adaptation. Our results are checked against individual-based simulations. We find that, compared to adaptation from *de-novo* mutations, (i) adaptation from standing variation proceeds by the fixation of more alleles of small effect; (ii) populations that adapt from standing genetic variation can traverse larger distances in phenotype space and, thus, have a higher potential for adaptation if the rate of environmental change is fast rather than slow.

INTRODUCTION

One of the biggest surprises that has emerged from evolutionary research in the past few decades is that, in contrast to what has been claimed by the neutral theory (KIMURA 1983), adaptive evolution at the molecular level is wide-spread. In fact, some empirical studies concluded that up to 45% of all amino acid changes between *Drosophila simulans* and *D. yakuba* are adaptive (SMITH and EYRE-WALKER 2002; ORR 2005b). Along the same line, WICHMAN *et al.* (1999) evolved the single-stranded DNA bacteriophage ΦX174 to high temperature and a novel host and found that $80 - 90\%$ of the observed nucleotide substitutions had an adaptive effect. These and other results have led to an increased interest in providing a formal framework for the adaptive process that goes beyond traditional population- and quantitative-genetic approaches and considers the statistical properties of suites of substitutions in terms of "individual mutations that have individual effects" (ORR 2005a). In general, selection following a change in the environmental conditions may act either on *de-novo* mutations or on alleles already present in the population, also known as standing genetic variation. Consequently, from the numerous studies that have attempted to address this subject, two complementary modelling approaches have emerged.

So-called adaptive-walk models (GILLESPIE 1984; KAUFFMAN and LEVIN 1987; ORR 2002, 2005b) typically assume that selection is strong compared to mutation, such that the population can be considered monomorphic all the time and all observed evolutionary change is the result of *de-novo* mutations. These models have produced several robust predictions (ORR 1998, 2000; MARTIN and LENORMAND 2006a,b), which are supported by growing empirical evidence (COOPER *et al.* 2007; ROCKMAN 2012; HIETPAS *et al.* 2013; but see BELL 2009), and has provided a statistical framework for the fundamental event during adaptation, that is, the substitution of a resident allele by a beneficial mutation. Specifically, the majority of models (e.g., GILLESPIE 1984; ORR 1998; MARTIN and LENORMAND 2006a) consider the effect-size distribution of adaptive substitutions following a sudden change in the environ-

4

ment. Recently, Kopp and Hermisson (2009b) and Matuszewski *et al.* (2014) extended this framework to gradual environmental change.

In contrast, most quantitative-genetic models consider an essentially inexhaustible pool of pre-existing standing genetic variants as the sole source for adaptation (Lande 1976). Evolving traits are assumed to have a polygenic basis, where many loci contribute small individual effects, such that the distribution of trait values approximately follows a Gaussian distribution (Bulmer 1980; Barton and Turelli 1991; Kirkpatrick *et al.* 2002). Since the origins of quantitative genetics lie in the design of plant and animal breeding schemes (Wricke and Weber 1986; Tobin *et al.* 2006; Hallauer *et al.* 2010), the traditional focus of these models was on predicting short-term changes in the population mean phenotype (often assuming constant genetic variances and covariances), and not on the fate and effect of individual alleles. The same is true for the relatively small number of models that have studied the contribution of new mutations in the response to artificial selection (e.g. Hill and Rasbash 1986a) and the shape and stability of the **G**-matrix (i.e., the additive variance-covariance matrix of genotypes; Jones *et al.* 2004, 2012).

It is only in the past decade that population geneticists have thoroughly addressed adaptation from standing genetic variation at the level of individual substitutions (Orr and Betancourt 2001; Hermisson and Pennings 2005; Chevin and Hospital 2008). Hermisson and Pennings (2005) calculated the probability of adaptation from standing genetic variation following a sudden change in the selection regime. They found that, for small-effect alleles, the fixation probability is considerably increased relative to that from new mutations. Furthermore, Chevin and Hospital (2008) showed that the selective dynamics at a focal locus are substantially affected by genetic background variation. These results where experimentally confirmed by Lang *et al.* (2011), who followed beneficial mutations in hundreds of evolving yeast populations and showed that the selective advantage of a mutation plays only a limited role in determining its ultimate fate. Instead, fixation or loss is largely determined by variation in the genetic background – which need not to be preexisting, but could quickly be

5

generated by a large number of new mutations. Still, predictions beyond these single-locus results have been verbal at best, stating that "compared with new mutations, adaptation from standing genetic variation is likely to lead to faster evolution [and] the fixation of more alleles of small effect [...]" (BARRETT and SCHLUTER 2008). Thus, despite recent progress, one of the central questions still remains unanswered: From the multitude of standing genetic variants segregating in a population, which are the ones that ultimately become fixed and contribute to adaptation, and how does their distribution differ from that of (fixed) *de-novo* mutations?

The aim of the present article is to contribute to overcoming what has been referred to as "the most obvious limitation" (ORR 2005b) of adaptive-walk models and to study the ecological and genetic factors that determine the genetic basis of adaptation from standing genetic variation. Specifically, we consider the evolution of a quantitative trait in a gradually changing environment. We develop an analytical framework that accurately describes the distribution of adaptive substitutions from standing genetic variation and discuss its dependence on the effective population size, the strength of selection and the rate of environmental change. In line with BARRETT and SCHLUTER (2008), we find that, compared to adaptation from *de-novo* mutations, adaptation from standing genetic variation proceeds, on average, by the fixation of more alleles of small effect. Furthermore, when standing genetic variation is the sole source for adaptation, faster environmental change can enable the population to remain better adapted and to traverse larger distances in phenotype space.

MODEL AND METHODS

Phenotype, Selection and Mutation

We consider the evolution of a diploid population of N individuals with discrete and non-overlapping generations characterized by a single phenotypic trait z, which is under Gaussian stabilizing selection with regard to a time-dependent optimum $z_{\mathrm{opt}}(t)$:

$$w(z,t) = \exp\left[-\frac{(z - z_{\mathrm{opt}}(t))^2}{2\sigma_s^2}\right], \tag{1}$$

where σ_s^2 describes the width of the fitness landscape. Throughout this paper we choose the linearly moving optimum,

$$z_{\mathrm{opt}}(t) = vt, \tag{2}$$

where v is the rate of environmental change.

Mutations enter the population at rate $\frac{\Theta}{2}$ (with $\Theta = 4Nu$ where u is the per-haplotype mutation rate), and we assume that their phenotypic effect size α follows a Gaussian distribution with mean 0 and variance σ_m^2 (which we will refer to as the distribution of new mutations), that is

$$p(\alpha) = \frac{1}{\sqrt{2\pi\sigma_m^2}} \exp\left(-\frac{\alpha^2}{2\sigma_m^2}\right). \tag{3}$$

Throughout this paper we equate genotypic with phenotypic values and, thus, neglect any environmental variance. Note that this model is, so far, identical to the moving-optimum model proposed by KOPP and HERMISSON (2009b) (see also BÜRGER 2000).

Genetic assumptions and simulation model

To study the distribution of adaptive substitutions from standing genetic variation, we con-

122 ducted individual-based simulations (IBS; available upon request; see BÜRGER 2000; KOPP

123 and HERMISSON 2009b) that explicitly model the simultaneous evolution at multiple loci,

124 while making additional assumptions about the genetic architecture of the selected trait, the

125 life cycle of individuals and the regulation of population size. This will serve as our main

126 model.

127 **Genome** Individuals are characterized by a linear (continuous) genome of diploid loci,

128 which determine the phenotype z additively (i.e., there is no phenotypic epistasis; note,

129 however, that there is epistasis for fitness). Mutations occur at constant rate $\frac{\Theta}{2N} = u$ per

130 haplotype. In contrast to the majority of individual-based models (e.g., JONES *et al.* 2004;

131 KOPP and HERMISSON 2009b; MATUSZEWSKI *et al.* 2014), we do not fix the number of

132 loci *a-priori*, but instead assume that each mutation creates a unique polymorphic locus,

133 whose position is drawn randomly from a uniform distribution over the entire genome (where

134 genome length is determined by the recombination parameter r described below). Thus, each

135 locus consists only of a wild-type allele with phenotypic effect 0 and a mutant allele with

136 phenotypic effect α, which is drawn from equation (3). Thus, we effectively design a bi-allelic

137 infinite-sites model with a continuum of alleles.

138 To monitor adaptive substitutions, we introduce a population-consensus genome $\mathcal{G}$ that keeps

139 track of all loci, that is, of all mutant alleles that are segregating in the population. If a

140 mutant allele becomes fixed in the population it is declared the new wild-type allele and its

141 phenotypic effect is reset to 0. The phenotypic effects of all fixed mutations are taken into

142 account by a variable z_{fix}, which can be interpreted as a phenotypic baseline effect. Thus,

143 the phenotype z of an individual i is given by

$$z_i = z_{\text{fix}} + \sum_{h \in \{1,2\}} \sum_{l \in \mathcal{G}} \mathbb{1}(i, l, h)\alpha_l.$$

144 where

8

$$\mathbb{1}(i,l,h) = \begin{cases} 1 & \text{if individual } i \text{ carries mutant allele } \alpha \text{ at locus } l \text{ on haplotype } h \\ 0 & \text{otherwise.} \end{cases}$$

Life cycle   Each generation, the following steps are performed:

1. *Viability selection:* Individuals are removed with probability $1 - w(z)$ (see eq. 1).

2. *Population regulation:* If, after selection, the population size N exceeds the carrying capacity K, $N - K$ randomly chosen individuals are removed.

3. *Reproduction:* The surviving individuals are randomly assigned to mating pairs, and each mating pair produces exactly $2B = 4$ offspring. Note that under this scheme, the effective population size N_e equals $4/3$ times the census size (BÜRGER 2000, p. 274). To account for this difference, Θ in the analytical approximations needs to calculated on the basis of this effective size, i.e., $\Theta = 4N_e u$. The offspring genotypes are derived from the parent genotypes by taking into account segregation, recombination and mutation.

Recombination   For each reproducing individual, the number of crossing-over events during gamete formation (i.e., the number of recombination breakpoints) is drawn from a Poisson distribution with (genome-wide recombination) parameter r (i.e., the total genome length is $r \cdot 100$cM, see Supporting Information 1). The genomic position of each recombination breakpoint is then drawn from a uniform distribution over the entire genome, and the offspring haplotype is created by alternating between the maternal and paternal haplotype depending on the recombination breakpoints. Free recombination (where all loci are assumed to be unlinked) corresponds to $r \to \infty$. In this case, for each locus a Bernoulli-distributed random number is drawn to determine whether the offspring haplotype will receive the maternal or the paternal allele at that locus.

9

165 **Simulation initialization and termination** Starting from a population of K wild-type

166 individuals with phenotype $z = 0$ (i.e., the population was perfectly adapted at $t = 0$),

167 we allowed for the establishment of genetic variation, σ_g^2, by letting the population evolve

168 for 10,000 generations under stabilizing selection with a constant optimum. Increasing the

169 number of generations had no effect on the average σ_g^2. Following this equilibration time, the

170 optimum started moving under ongoing mutational input, and the simulation was stopped

171 once all alleles from the standing genetic variation had either been fixed or lost (i.e., when

172 $\sigma_{sgv}^2 = 0$). Simulations were replicated until a total number of 5000 adaptive substitutions

173 from standing genetic variation was recorded.

174 **Analytical approximations: Evolution of a focal locus in the presence of genetic**

175 **background variation**

176 In order to obtain an analytically tractable model, we need to approximate the multi-locus

177 dynamics. Clearly, simple interpolation of single locus theory will fail, because when alleles

178 at different loci influencing the same trait segregate in the standing genetic variation, the

179 selective dynamics of any individual allele are critically affected by the collective evolutionary

180 response at other loci. In particular, any allele that brings the mean phenotype closer to the

181 optimum simultaneously decreases the selective advantage of other such alleles (epistasis for

182 fitness). Thus, if simultaneous evolution at many loci allows the population to closely follow

183 the optimum, large-effect alleles at any given locus are likely to remain deleterious (as their

184 carriers would overshoot the optimum). To account for these effects, we adopt a quantitative-

185 genetics approach originally developed by LANDE (1983) and introduce a genetic background

186 z_B that evolves according to Lande's equation

$$\Delta \bar{z} = \sigma_g^2 \beta, \tag{5a}$$

187 where

$$\beta = \frac{\partial \log(\bar{w})}{\partial \bar{z}} \tag{5b}$$

denotes the selection gradient, which measures the change in log mean fitness per unit change of the mean phenotype and σ_g^2 gives the genetic variance (LANDE 1976). Furthermore, assuming that the distribution of phenotypic values from the genetic background is Gaussian and the genetic variance remains constant, the mean background phenotype evolves according to

$$\bar{z}_{\mathrm{B}}(t) \approx vt - \frac{v}{\gamma}(1 - (1 - \gamma)^t) \tag{6a}$$

with

$$\gamma = \frac{\sigma_g^2}{\sigma_g^2 + \sigma_s^2} \tag{6b}$$

(BÜRGER and LYNCH 1995).

Given the dynamics of the genetic background, we choose one focal locus and derive the time-dependent selection coefficient $s(\alpha, t)$ for an allele with phenotypic effect α (for details see below). We then use theory for adaptation from standing genetic variation (HERMISSON and PENNINGS 2005) and for fixation under time-inhomogeneous selection (UECKER and HERMISSON 2011) to estimate the fixation probability for this allele (see also Appendix 1). As long as there is no linkage (i.e., there is free recombination between *all* loci), each locus can be viewed as the focal locus (with a specific phenotypic effect α), allowing us to get an estimate for the overall distribution of adaptive substitutions from standing genetic variation. Thus, in these approximations, our multi-locus model is effectively treated within a single-locus framework. Note that a similar focal-locus approach has recently been used to analyze the effect of genetic background variation on the trajectory of an allele sweeping to fixation (CHEVIN and HOSPITAL 2008), and to study the probability of adaptation to novel

11

207 environments (GOMULKIEWICZ *et al.* 2010), with both studies stressing the fact that genetic

208 background variation cannot be neglected and critically affects the adaptive outcome.

Wright-Fisher simulations: A focal locus with recurrent mutations

210 To simulate evolution at a focal locus, we followed HERMISSON and PENNINGS (2005) and

211 implemented a multinomial Wright-Fisher (WF) sampling approach (available upon request).

212 These simulations serve as an additional analysis tool that has been adjusted to the approx-

213 imation method and allows the adaptive process to be simulated fast and efficiently. In

214 addition, they go beyond the individual-based model in one aspect, as they do not make the

215 infinite-sites assumption but allow for recurrent mutation at the focal locus.

216 **Genome** At the focal locus, mutations with a fixed allelic effect α appear recurrently

217 at rate θ and convert ancestral alleles into derived mutant alleles. Accordingly, despite a

218 genetic background with normally distributed genotypic values, there are at most two types

219 of (focal) alleles in the population, where each type "feels" only the mean background $\bar{z}_{\mathrm{B}}$,

220 which evolves according to Lande's equation (eq. 5, see above). The genetic background

221 variation σ_g^2 is assumed to be constant and serves as a free parameter that is independent of

222 θ, N_e and σ_s^2. Note that the evolutionary response at the focal locus is influenced by that of

223 the genetic background, and vice versa, meaning that the two are interdependent.

224 **Procedure** We follow the evolution of $2N_e$ alleles at the focal locus. Each generation is

225 generated by multinomial sampling, where the probability of choosing an allele of a given type

226 (ancestral or derived) is weighted by its respective (marginal) fitness. Furthermore, the mean

227 phenotype of the genetic background $\bar{z}_{\mathrm{B}}$ evolves deterministically according to equation (5)

228 with constant σ_g^2. To let the population reach mutation-selection-drift equilibrium, each

229 simulation is started $4N_e$ generations before the environment starts changing. Initially, the

230 population consists of only ancestral alleles "0"; the derived allele "1" is created by mutation.

12

₂₃₁ If the derived allele reaches fixation before the environmental change (by drift), it is itself

₂₃₂ declared "ancestral"; i.e., the population is set back to the initial state. After $4N_e$ generations,

₂₃₃ the optimum starts moving, such that the selection coefficient of the derived allele, which is

₂₃₄ initially deleterious (i.e., $s(\alpha, t) \leq 0$), increases and may eventually become beneficial (i.e.,

₂₃₅ $s(\alpha, t) > 0$), depending on the response at the genetic background. Simulations continue until

₂₃₆ the derived allele is either fixed or lost. Fixation probabilities are estimated from 100,000

₂₃₇ simulation runs.

₂₃₈ Both simulation programs are written in C++ and make use of the Gnu Scientific Library

₂₃₉ (GALASSI *et al.* 2009). Mathematica (Wolfram Research, Inc., Champaign, USA) was used

₂₄₀ for the numerical evaluation of integrals and to create plots and graphics, making use of the

₂₄₁ LevelScheme package (CAPRIO 2005).

₂₄₂ A summary of our notation is given in Table 1.

Table 1 – A summary of notation and definitions.

α	phenotypic effect of mutation
$p(\alpha)$	(Gaussian) distribution of new mutations
z	phenotype
$\bar{z}_{\mathrm{B}}$	mean genetic background phenotype
v	rate of environmental change
$w(z, z_{opt}(t))$	(Gaussian) fitness function
σ_s^2	width of Gaussian fitness function
σ_m^2	variance of new mutations
σ_g^2	(background) genetic variance
$s(\alpha, t)$	time-dependent selection coefficient for allele with phenotypic effect α
x	frequency of mutant allele
N_e	effective population size
θ	per locus mutation rate
Θ	population-wide mutation rate (per trait)
Π_{fix}	fixation probability
$\rho(x, \alpha)$	Distribution of mutant allele frequency at a single locus with phenotypic effect α
P_{SGV}	Probability to adapt from standing genetic variation
p_{SGV}	Distribution of adaptive substitutions from standing genetic variation
δ_{eq}	equilibrium lag

RESULTS

243 In the following, we calculate, first, the probability that a focal allele from the standing genetic

244 variation becomes fixed when the population adapts to a moving phenotypic optimum, and

245 second, the effect-size distribution of such alleles. Note that the first result will be derived

246 under the assumption of recurrent mutation (see "Wright-Fisher simulations"), and serves

247 as an intermediate step for the second result, which is based on an infinite-sites model (see

248 "Genetic assumptions and simulation model").

249 **The probability for adaptation from standing genetic variation**

250 The probability that a focal mutant allele from the standing genetic variation contributes to

251 adaptation depends on the dynamics of its the selection coefficient in the presence of genetic

252 background variation. For an allele with effect α and a genetic background with mean $\bar{z}_{\mathrm{B}}$

253 and variance σ_g^2, the selection coefficient can be calculated as

$$
\begin{aligned}
s(\alpha, t) &= \frac{w(\alpha + \bar{z}_{\mathrm{B}}(t), t)}{w(\bar{z}_{\mathrm{B}}(t), t)} - 1 \\
&\approx -\frac{\alpha^2}{2\left(\sigma_s^2 + \sigma_g^2\right)} + \frac{\alpha}{\sigma_s^2 + \sigma_g^2}(vt - \bar{z}_{\mathrm{B}}(t)).
\end{aligned}
\tag{7}
$$

254 Note that the genetic background variance has the effect of broadening the fitness landscape

255 experienced by the focal allele (the term $\sigma_s^2 + \sigma_g^2$).

Plugging equation (6a) into equation (7) then yields the selection coefficient,

$$
s(\alpha, t) \approx -\frac{\alpha^2}{2\left(\sigma_s^2 + \sigma_g^2\right)} + \frac{\alpha v}{\gamma\left(\sigma_s^2 + \sigma_g^2\right)}(1 - (1 - \gamma)^t).
\tag{8}
$$

256 Assuming that the population is perfectly adapted at $t = 0$ ($\bar{z}_B = 0$), the initial (deleterious)

257 selection coefficient is given by

14

$$s(\alpha, 0) = -\frac{\alpha^2}{2\left(\sigma_s^2 + \sigma_g^2\right)}.$$

Unlike in the model without genetic background variation (KOPP and HERMISSON 2009b), $s(\alpha, t)$ does not increase linearly, but instead depends on the evolution of the phenotypic lag δ between the optimum and the mean background phenotype. In particular, the population will reach a dynamic equilibrium with $\Delta \bar{z}_\mathrm{B} = v$, where it follows the optimum with a constant lag

$$\delta_\mathrm{eq} = \frac{v}{\gamma} \tag{9}$$

(BÜRGER and LYNCH 1995). Consequently, the selection coefficient for α approaches

$$\lim_{t \to \infty} s(\alpha, t) = -\frac{\alpha^2}{2\left(\sigma_s^2 + \sigma_g^2\right)} + \frac{\alpha v}{\gamma\left(\sigma_s^2 + \sigma_g^2\right)}. \tag{10}$$

Note that the right-hand side can be written as $s(\alpha, 0) + \alpha\beta_\mathrm{eq}$, where β_eq is the equilibrium selection gradient (KOPP and MATUSZEWSKI 2014). In this case, the largest obtainable selection coefficient is for $\alpha = \delta_\mathrm{eq}$ and evaluates to

$$s_\mathrm{max} = s(\delta_\mathrm{eq}, \infty) = \frac{v^2}{2\gamma^2\left(\sigma_s^2 + \sigma_g^2\right)}. \tag{11}$$

The range of allelic effects α that can reach a positive selection coefficient is bounded by $\alpha_\mathrm{min} = 0$ and $\alpha_\mathrm{max} = 2\delta_\mathrm{eq}$. Note that in previous adaptive-walk models (e.q., KOPP and HERMISSON 2009b; MATUSZEWSKI *et al.* 2014) there was no strict α_max, since the population followed the optimum by stochastic jumps, whereas in the present model, the genetic background evolves deterministically and establishes a constant equilibrium lag.

Assuming that α was deleterious prior to the environmental change, its allele frequency spectrum $\rho(x, \alpha)$ is given by equation (A5). When genetic background variation is absent

274 the fixation probability $\Pi_{\text{fix}}(\alpha)$ (eq. A7) can be calculated explicitly using

$$\varphi_{\sigma_g^2=0}(\alpha) = 1 + \frac{1}{2}\sqrt{\frac{\pi}{2\frac{\alpha v}{\sigma_s^2}}}\exp\left(\frac{s(\alpha,0)^2}{2\frac{\alpha v}{\sigma_s^2}}\right)\text{erfc}\left(\frac{s(\alpha,0)}{\sqrt{2\frac{\alpha v}{\sigma_s^2}}}\right). \tag{12}$$

275 For the general case, however, $\Pi_{\text{fix}}(\alpha)$ can only be calculated numerically using equation (8)

276 in equation (A7b), yielding

$$2\varphi(\alpha) = 1 + \int_0^\infty (1+s(\alpha,t))\exp\left[-\left(\left(-\frac{\alpha^2}{2\left(\sigma_s^2+\sigma_g^2\right)}\right) + \left((1-(1-\gamma)^t)\frac{1}{\log[(1-\gamma)^t]}+1\right)\frac{\alpha v}{\gamma\left(\sigma_s^2+\sigma_g^2\right)}\right)t\right]\mathrm{d}t. \tag{13}$$

277 The fixation probability for an allele from the standing genetic variation with allelic effect α

278 and a recurrent (per locus) mutation rate θ can then be calculated as

$$P_{\text{SGV}}(\alpha) = \begin{cases} 1 - C(\alpha)\int_0^1 x^{\theta-1}\exp[-4N_e|s(\alpha,0)|x]\left(1-\frac{1}{\varphi(\alpha)}\right)^{2N_e x}\mathrm{d}x & \text{if } 0<\alpha<\alpha_{max} \\ 0 & \text{otherwise,} \end{cases} \tag{14}$$

279 where $C(\alpha) = \left(\frac{\gamma[\theta,4N_e|s(\alpha,0)|]}{(4N_e|s(\alpha,0)|)^\theta}\right)^{-1}$.

280 When checked against Wright-Fisher simulations (see Methods for details), our analytical

281 approximation equation (14) performs generally very well (Figs. 1 and S3_1). The only

282 exception occurs when the background variation is high (large σ_g^2) and stabilizing selection

283 is weak (i.e., if σ_s^2 is large). In this case, equation (14) underestimates $P_{\text{SGV}}(\alpha)$ for small

284 $\alpha \sim 0.5\sigma_m$. The reason is that, under a constant optimum (i.e., before the environmental

285 change), the genetic background compensates for the deleterious effect of α (i.e., $\bar{z}_{\text{B}} < 0$,

286 in violation of our assumption that $\bar{z}_{\text{B}}(0) = 0$), effectively reducing the selection strength

287 against the deleterious mutant allele. Consequently, α is, on average, present at higher

288 initial frequencies than predicted by equation (A5).

289 Note that, if α is small compared to the genetic background variation (i.e., in the limit of

16

290    $\alpha/\sigma_m \to 0$) and environmental change is slow (i.e., $v \ll 10^{-5}$), $P_{\text{SGV}}(\alpha)$ will approach the

291   probability of fixation from standing genetic variation for a neutral allele (i.e., $\alpha = 0$), which

292   can be calculated as

$$P_{\text{SGV, neutral}} = \int_0^1 x\rho(x)\mathrm{d}x = \frac{H_\theta - 1}{\gamma + \psi(\theta)}. \tag{15}$$

293   where $\rho(x)$ is given by equation (A3), H_n denotes the nth harmonic number, $\gamma \approx 0.577$ is

294   Euler's gamma and $\psi(\cdot)$ is the polygamma function (see dashed lines in Figs. 1 and S3_1).

295   Figures 1 and S3_1 show some general trends: First, the probability for a mutant allele to

296   become fixed increases with the rate of environmental change, v, (irrespective of its effect

297   size α, the per locus mutation rate θ and the width of the fitness landscape σ_s^2) since only

298   the positive term in equation (8) depends (linearly) on v. Second, $P_{\text{SGV}}(\alpha)$ is proportional

299   to θ as long as θ is small (compare $\theta = 0.004$ and $\theta = 0.04$ in Fig. S3_1), simply because the

300   probability that α is present in the population is linear in θ. Thus, Figure 1 is representative

301   for the limit $\theta \to 0$ which will be used below. Indeed, only if the per-locus mutation rate

302   is fairly large ($\theta > 0.1$), does the shape of the distribution of allele frequencies become

303   important, and the increase in $P_{\text{SGV}}(\alpha)$ with θ becomes less than linear (Fig. S3_1). Third,

304   changes in the width of the fitness landscape, σ_s^2, have a dual effect: While increasing σ_s^2

305   promotes the initial frequency of the focal allele in the standing genetic variation (because

306   stabilizing selection is weaker), the selection coefficient increases more slowly after the onset

307   of environmental change (such that the allele is less likely to be picked up by selection;

308   see eq. 7). Our results, however, show that the former effect always outweighs the latter

309   (as $P_{\text{SGV}}(\alpha)$ increases with σ_s^2). Finally, if the genetic background variation σ_g^2 is below

310   a threshold value (e.g., $\sigma_g^2 < 0.005$; the exact threshold should depend on θ and σ_s^2) it

311   only marginally affects the fixation probability of the focal allele α. Once σ_g^2 surpasses this

312   value, however, it critically affects $P_{\text{SGV}}(\alpha)$ (in accordance with the results by CHEVIN and

17

313 HOSPITAL 2008). In particular, as σ_g^2 increases $P_{\mathrm{SGV}}(\alpha)$ decreases, because most large-effect

314 alleles remain deleterious even if environmental change is fast. Thus, enlarged background

315 variation acts as if reducing the rate of environmental change v. In summary, our analytical

316 results are in good agreement with the WF-simulation model, and will serve as an important

317 first step towards deriving the distribution of adaptive substitutions from standing genetic

318 variation.

Figure 1 – The probability for a mutant allele to adapt from standing genetic variation as a function of the rate of environmental change v. Solid lines correspond to the analytical prediction (eq. 14), the grey dashed line shows the probability for a neutral allele ($\alpha = 0$; eq. 15), and symbols give results from Wright-Fisher simulations. The phenotypic effect size α of the mutant allele ranges from $0.5\sigma_m$ (top line; black) to $3\sigma_m$ (bottom line; purple) with increments of $0.5\sigma_m$. The figures in each parameter box (per locus mutation rate θ, width of fitness landscape σ_s^2) correspond to different values of the genetic background variation σ_g^2 with $\sigma_g^2 = 0$ (no background variation; top left), $\sigma_g^2 = 0.005$ (top right), $\sigma_g^2 = 0.01$ (bottom left) and $\sigma_g^2 = 0.05$ (bottom right). Other parameters: $N_e = 25000$, $\theta = 0.004$, $\sigma_m^2 = 0.05$.

319
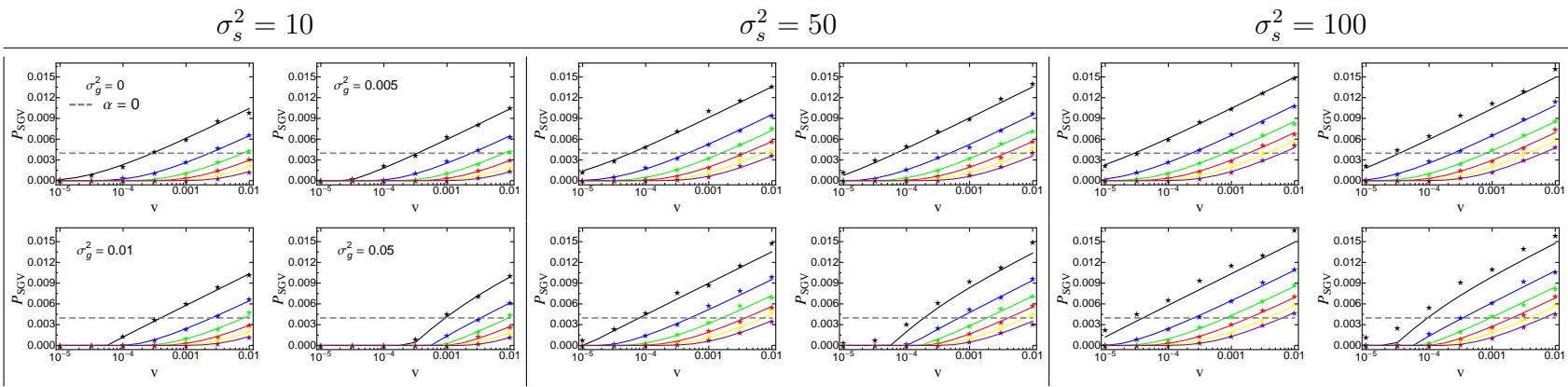
320

19

The distribution of adaptive substitutions from standing genetic variation

We now derive the distribution of adaptive substitutions from standing genetic variation over all mutant effects α. In the previous section, we derived the fixation probability at a focal locus (with a given effect α) by treating the genetic background variance σ_g^2 as an independent model parameter. In the full model, this variance results from a balance of mutation, selection and drift at all background loci. As such, it is a function of the basic model parameters for these forces. Since we use an infinite-sites model, there is no recurrent mutation and each allele originates from a single mutation. Consequently, the amount of background variation σ_g^2 is accurately predicted by the Stochastic-House-of-Cards (SHC) approximation (not shown; BÜRGER and LYNCH 1995)

$$\sigma_g^2 = \frac{\Theta \sigma_m^2}{1 + \frac{N_e \sigma_m^2}{\sigma_s^2}}, \tag{16}$$

where mutation is parametrized by the total (per trait) mutation rate Θ and the mutational variance σ_m^2, the width of the fitness landscape is given by σ_s^2, and the effective population size N_e is a measure for genetic drift.

To derive the probability that an allele with a given phenotypic effect α contributes to adaptation, we first need to calculate the probability that such an allele segregates in the population at time 0. Following HERMISSON and PENNINGS (2005), the probability P_0 that the allele is *not* present can be approximated by integrating over the distribution of allele frequencies $\rho(x, \alpha)$ (eq. A5) from 0 to $\frac{1}{2N_e}$ yielding

$$P_0(\alpha) \approx \left(\frac{2N_e}{4N_e|s(\alpha,0)|+1} \right)^{-\theta}$$
$$= \exp \left[-\theta \log \left[\frac{2N_e}{4N_e|s(\alpha,0)|+1} \right] \right] \tag{17}$$

20

339   (eq. 7 and Appendix of HERMISSON and PENNINGS 2005). The fixation probability can then

340   be calculated by conditioning on segregation of the allele in the limit $\theta \to 0$ (due to the

341   infinite-sites assumption). Using equation (14), this probability reads

$$
\begin{aligned}
\Pi_{\mathrm{seg}}(\alpha) &= \lim_{\theta \to 0} \frac{P_{\mathrm{SGV}}(\alpha)}{1 - P_0(\alpha)} \\
&\approx \lim_{\theta \to 0} \frac{1 - C(\alpha) \int_0^1 x^{\theta-1} \exp[-4N_e|s(\alpha,0)|x] \left(1 - \frac{1}{\varphi(\alpha)}\right)^{2Nx} \mathrm{d}x}{1 - \exp\left[-\theta \log\left[\frac{2N_e}{4N_e|s(\alpha,0)|+1}\right]\right]},
\end{aligned}
\tag{18}
$$

342   where $C(\alpha) = \left(\frac{\gamma[\theta, 4N_e|s(\alpha,0)|]}{(4N_e|s(\alpha,0)|)^\theta}\right)^{-1}$ (see also eq. A5) and with $\varphi(\alpha)$ according to equation (13).

343   The limit in equation (18) can be approximated numerically by setting θ to a very small, but

344   positive value.

345   Multiplying by the rate of mutations with effect α (i.e., $\Theta p(\alpha)$), the distribution of adaptive

346   substitutions from standing genetic variation is given by

$$
\begin{aligned}
p_{\mathrm{SGV}}(\alpha) &\approx \frac{\Theta p(\alpha) \Pi_{\mathrm{seg}}(\alpha)}{\int_0^{\alpha_{max}} \Theta p(\alpha) \Pi_{\mathrm{seg}}(\alpha) \mathrm{d}\alpha} \\
&= C_1(\alpha) p(\alpha) \Pi_{\mathrm{seg}}(\alpha),
\end{aligned}
\tag{19}
$$

347   where $C_1(\alpha)$ is a normalization constant (black line in Figs. 2, 3 and Fig. 4). Note that

348   equation (19) still depends on Θ through its effect on the background variance σ_g^2 (which

349   affects $\Pi_{\mathrm{seg}}(\alpha)$). In particular, in the SHC approximation (eq. 16), σ_g^2 scales linearly with Θ.

350   Furthermore, equation (19) should be valid for any distribution of mutational effects $p(\alpha)$.

351   In the limit where the equilibrium lag is reached fast (i.e., when γ is large; eq. 6b), the

352   moving-optimum model reduces to a model with constant selection for any focal allele (i.e., as

353   in HERMISSON and PENNINGS 2005). Using equations (A6) and (17) the fixation probability

21

354 for a segregating allele can be calculated as

$$\Pi_{\text{seg,SGV},\delta_{\text{eq}}}(\alpha) \approx \lim_{\theta \to 0} \frac{1 - \exp\left[-\theta \log\left[1 + \frac{4N_e s(\alpha,\infty)}{4N_e |s(\alpha,0)| + 1}\right]\right]}{1 - P_0(\alpha)}. \tag{20}$$

355 Plugging equation (20) into equation (19), the distribution of adaptive substitutions from

356 standing genetic variation can be approximated by

$$p_{\text{SGV},\delta_{\text{eq}}}(\alpha) \approx C_2(\alpha) p(\alpha) \Pi_{\text{seg,SGV},\delta_{\text{eq}}}(\alpha), \tag{21}$$

357 where $C_2(\alpha)$ is a normalization constant (red line in Figs. 2, 3).

358 Similarly, the fixation probability of *de-novo* mutations under the equilibrium lag δ_{eq} can be

359 derived (using 11 and eq. A2 with an initial frequency of $1/(2N)$) as

$$\Pi_{\text{fix,DNM},\delta_{\text{eq}}}(\alpha) = \left(1 - \exp\left[-\frac{\alpha(2\delta_{\text{eq}} - \alpha)}{\sigma_s^2 + \sigma_g^2}\right]\right), \tag{22}$$

360 yielding the distribution of adaptive substitutions

$$p_{\text{DNM},\delta_{\text{eq}}}(\alpha) \approx p(\alpha) C_3(\alpha) \Pi_{\text{fix,DNM},\delta_{\text{eq}}}(\alpha), \tag{23}$$

361 where $C_3(\alpha)$ is a normalization constant (grey curve in Figs. 2, 3).

362 In contrast, if the environment changes very slowly, we can calculate the limit distribution of

363 adaptive substitutions from standing genetic variation by approximating the fixation proba-

364 bility by that of a neutral allele (i.e., its allele frequency x). In this case,

$$\Pi_{\text{seg},v \to 0}(\alpha) \approx \lim_{\theta \to 0} \frac{\mathcal{F}(\alpha)}{1 - P_0(\alpha)} \tag{24a}$$

365 with

22

$$\mathcal{F}(\alpha) = \int_0^1 \rho(x, \alpha) x \mathrm{d}x = \frac{{}_1F(0, \theta + 1, 4N_e|s(\alpha, 0)|)_1}{{}_1F(0, \theta, 4N_e|s(\alpha, 0)|)_1}, \tag{24b}$$

366 where $\rho(x, \alpha)$ is given by equation (A4) and the right-hand side is a ratio of hypergeometric

367 functions.

368 Using equation (24a) the distribution of substitutions from standing genetic variation reads

$$p_{\mathrm{SGV}, v \to 0}(\alpha) \approx C_4(\alpha) p(\alpha) \Pi_{\mathrm{seg}, v \to 0}(\alpha), \tag{25}$$

369 where $C_4(\alpha)$ again denotes a normalization constant (blue line in Figs. 3, S3_2).

370 **The accuracy of the approximation** When compared to individual-based simulations,

371 our analytical approximation for the distribution of adaptive substitutions from standing

372 genetic variation (eq. 19) performs, in general, very well as long as selection is strong, that is,

373 the rate of environmental change v is high and/or the width of the fitness landscape σ_s^2 is not

374 too large (Fig. 2). Under weak selection, however, equation (19) fails to capture the fixation

375 of alleles with neutral or negative effects ("backward fixations"; $\alpha \leq 0$). The reason is that

376 equation (A7) only considers the fixation of alleles whose selection coefficient $s(\alpha, t)$ becomes

377 positive in the long term. But if the rate of environmental change is slow (or σ_s^2 is very

378 large), most alleles get fixed or lost simply by chance, that is, genetic drift. In particular, if

379 genetic drift is the main driver of phenotypic evolution (i.e., $N_e|s(\alpha, t)| < 1$), the distribution

380 of adaptive substitutions is almost symmetric around 0 (see Fig. S3_2). This distribution

381 is described very well by equation (25), which assumes that the fixation probability of an

382 allele is proportional to its initial frequency in the standing variation. In addition, even

383 for cases where environmental change imposes modest directional selection, equation (25)

384 still captures the shape of the distribution of adaptive substitutions reasonably well, when

385 centered around the empirical mean (blue line in Figs. 2, 3).

Figure 2 – The distribution of adaptive substitutions from standing genetic variation. Histograms show results from individual-based simulations. The black line corresponds to the analytical prediction (eq. 19), with the genetic background variation σ_g^2 determined by the SHC approximation (eq. 16). The red line gives the analytical prediction for the limiting case where the equilibrium lag δ_{eq} is reached fast (eq. 21). The blue line is based on the analytical prediction eq. (25) – which assumes a neutral fixation probability – but has been shifted so that it is centered around the empirical mean. The grey curve gives the analytical prediction for substitutions from *de-novo* mutations under the assumption that the phenotypic lag δ_{eq} has reached its equilibrium (eq. 23). The asterisks indicate where $N_e s_{max} \geq 10$. Fixed parameter: $\sigma_m^2 = 0.05$.
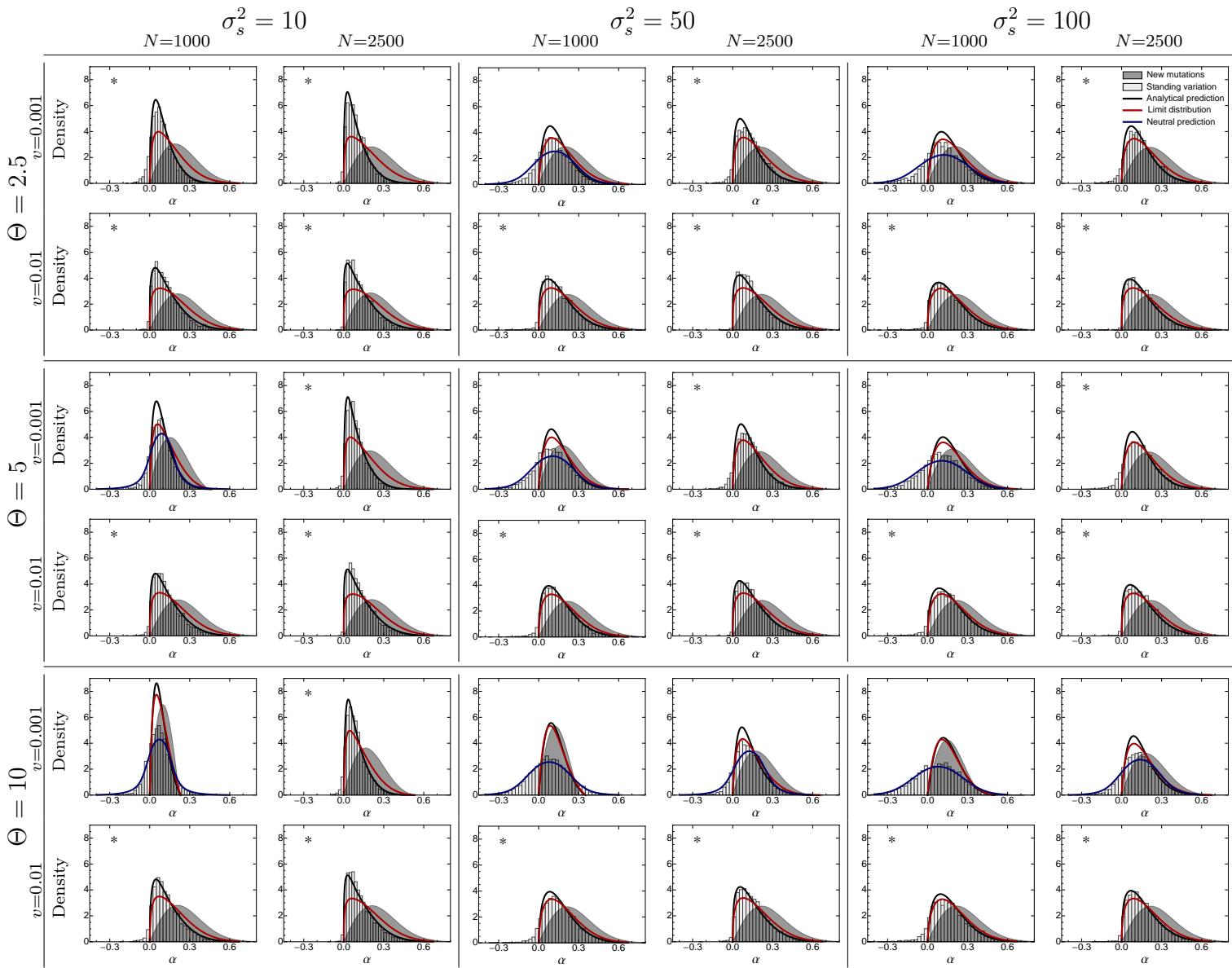
Figure 3 – The distribution of adaptive substitutions from standing genetic variation for various rates of environmental change. For further details see Fig. 2. Fixed parameters: $\Theta = 2.5$, $N = 2500$, $\sigma_m^2 = 0.05$.
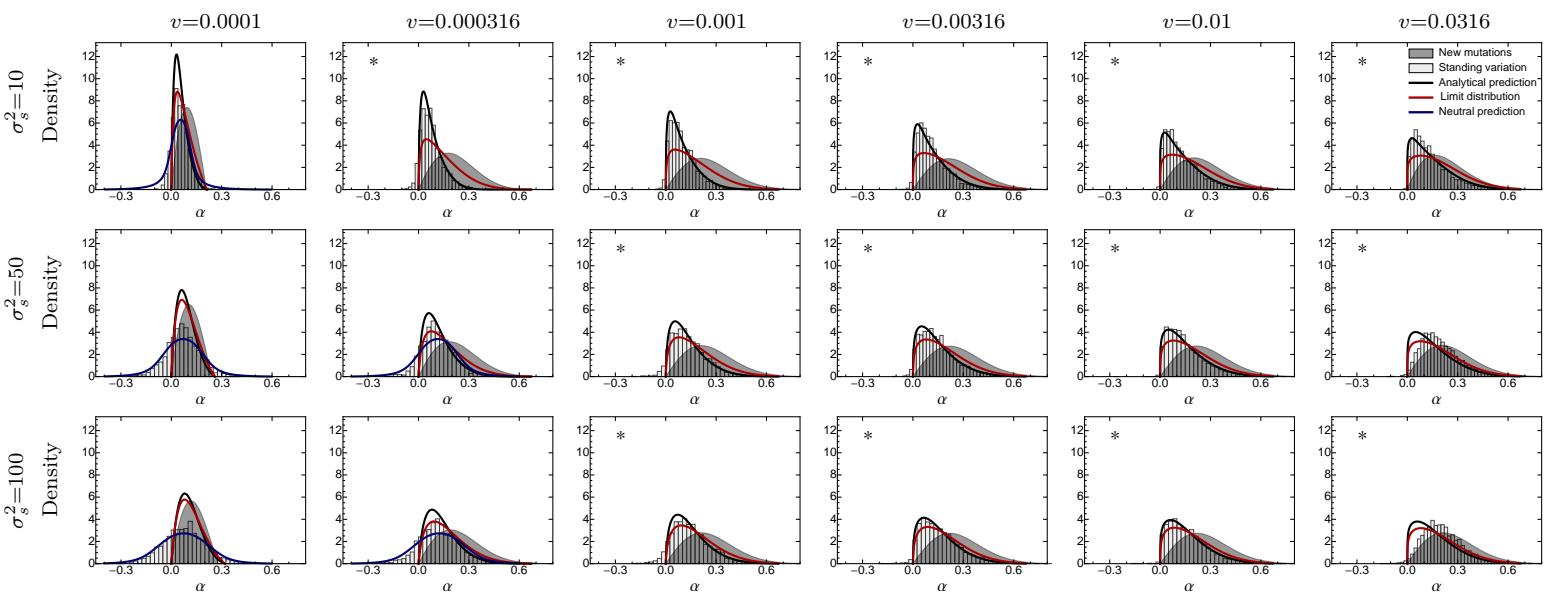
386 With a moving phenotypic optimum, the selection coefficient (eq. 8) is initially very small.

387 Accordingly, there is always a phase during the adaptive process where genetic drift domi-

388 nates, that is, where $N_e|s(\alpha,t)| < 1$ for all mutant alleles. The length of this phase (i.e., the

389 time it takes until selection becomes the main force of evolution) depends on the interplay of

390 multiple parameters, notably v, σ_s^2, N_e and Θ. A good heuristic to determine whether evo-

391 lution will ultimately become dominated by selection is to calculate $N_e s_{\max}$ (eq. 11), which

392 gives the maximal population-scaled selection coefficient. Since the selection coefficient of

393 most mutations will be smaller than this value, one can consider as a rule of thumb that

394 selection is the main driver of evolution as long as $N_e s_{\max} \geq 10$. In this case, equation (19)

395 matches the individual-based simulations very well (see asterisks in Figs. 2, 3). In summary,

400 the accuracy of our approximation crucially depends on the efficacy of selection.

401 The effects of linkage on the distribution of adaptive substitutions from standing genetic

402 variation are discussed in Supporting Information 1. The main result is that only tight

403 linkage has a noticeable effect, namely to reduce the efficacy of selection and increase the

404 proportion of "backward" fixations (moving the distribution closer to the prediction from

405 eq. 25).

406 **Biological interpretation** As shown in Figures (2) and (3), adaptive substitutions from

407 standing genetic variation have, on average, smaller phenotypic effects than those from *de-*

408 *novo* mutations. There are two reasons for this result. First, in the standing genetic variation,

409 small-effect alleles are more frequent than large-effect alleles and might already segregate

410 at appreciable frequency (increasing their fixation probability). Second, substitutions from

411 standing variation occur in the initial phase of the adaptive process, where the phenotypic

412 lag is small, whereas our approximation for *de-novo* mutations (eq. 23) assumes that the phe-

413 notypic lag has reached its maximal (equilibrium) value (which need not be large, depending

414 on the amount of genetic background variation). The relative importance of these two effects

415 can be seen in Figures (2) and (3): Comparing the grey shaded area (eq. 23; *de-novo* muta-

416 tions under the equilibrium lag) with the red line (eq. 21; standing genetic variation under

417 the equilibrium lag) shows the effect of larger starting frequencies of small-effect mutations

418 from the standing genetic variation. The difference of the black (eq. 19; standing genetic

419 variation) and red (eq. 21; standing genetic variation under the equilibrium lag) lines show

420 the effects of the initially smaller lag (i.e., the effect of the dynamical selection coefficient).

421 Note that the first effect is always important (even if Θ and σ_s^2 are large and v is small, where

422 the red line and the grey curve almost coincide—though this is only because the approxima-

423 tion is bad). The second effect, however, becomes particularly important if $\gamma = \sigma_g^2/(\sigma_g^2 + \sigma_s^2)$

424 is small (i.e, if the time to reach the equilibrium lag is large), such that selection coefficients

425 are dynamic and small-effect alleles are selected earlier than large-effect alleles, explaining

426 the relative lack of large-effect alleles in the distribution of adaptive substitutions.

427 Generally, the distribution of adaptive substitutions is unimodal and generally resembles a

428 log-normal distribution (Figs. 2, 3). Only if selection is very weak (i.e., when σ_s^2 is large

429 and/or v is small), does it contain a significant proportion of "backward fixations" (with

430 negative α; Fig. 3; see "Accuracy of the Approximation"). As the rate of environmental

431 change v increases, the mean phenotypic effect of substitutions increases (Fig. 4, top row),

432 too, but the mode may actually decrease (Fig. 3), that is, the distribution becomes more

433 asymmetric and skewed, resembling the "almost exponential" distribution of substitutions

434 from *de-novo* mutations in the sudden change scenario (ORR 1998). A likely explanation

435 is that small-effect alleles, which are common in the standing variation, are under stronger

436 selection and have an increased fixation probability if v is large (see Fig. 1).

437 Interestingly, if the environment changes very fast the simulated distribution of adaptive

438 substitutions from standing genetic variation almost exactly matches the one predicted by

439 equation (23) for *de-novo* mutations (Fig. 5, see also Figs. 2, 3). However, this seems to be an

440 artefact rather than a relevant biological phenomenon. The reason is that the environment

441 changes so fast that the population quickly dies out. Thus, the resulting distribution of

442 adaptive substitutions is that for a dying population and might not necessarily reflect the

27

443 adaptive process. In an experimental setup, though, where populations evolve until they

444 go extinct, the distribution of adaptive substitutions from standing genetic variation might

445 truly be indistinguishable from that from *de-novo* mutations.
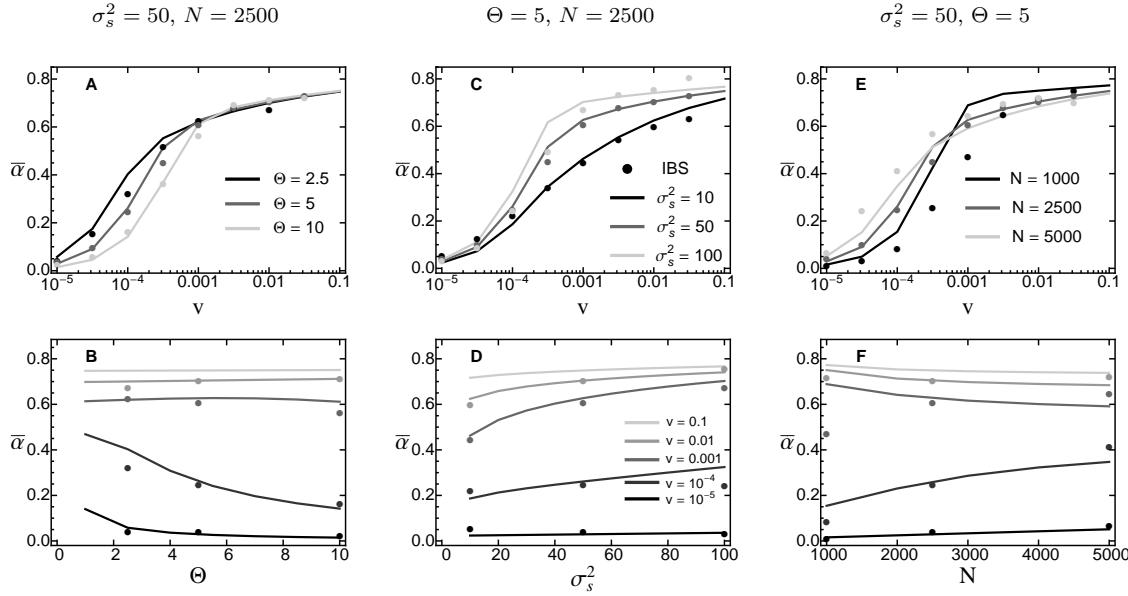
Figure 4 – The mean size of adaptive substitutions from standing genetic variation, measured in units of mutational standard deviations (σ_m) as a function of the rate of environmental change v (top row) and for various v as a function of the population-wide mutation rate Θ (bottom left), the width of the fitness landscape σ_s^2 (bottom middle) and the population size N (bottom right). Lines show the analytical prediction (the mean of the distribution eq. eq:pDistMoveOpt), and symbols give results from individual-based simulations. Error bars for standard errors are contained within the symbols. For $v = 0.1$, no simulation results are shown, as these constitute a degenerate case (for details see "The accuracy of the approximation"). Fixed parameter: $\sigma_m^2 = 0.05$.

446
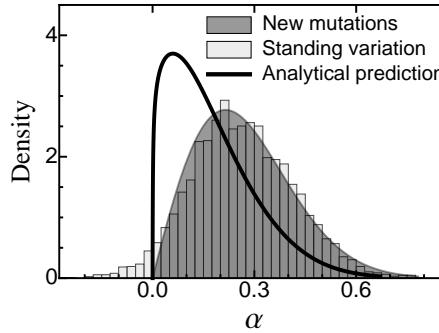
Figure 5 – The distribution of adaptive substitutions from standing genetic variation in the case of fast environmental change. For further details see Fig. 2. Fixed parameters: $\sigma_s^2 = 100$, $\Theta = 10$, $N = 2500$, $v = 0.1$, $\sigma_m^2 = 0.05$.

447

448 In the following, we discuss the influence of the other model parameters (Θ, σ_s^2 and N) on

449 the distribution of adaptive substitutions from standing genetic variation, and in particular,

28

450 its mean $\bar{\alpha}$ (Fig. 4).

451 The effect of the rate of mutational supply Θ depends strongly on the rate of environmental

452 change v: $\bar{\alpha}$ decreases with Θ if v is small but is independent of Θ if v is large (Fig. 4B).

453 Recall that Θ enters $p_{\mathrm{SGV}}(\alpha)$ (eq. 19) only indirectly through the background variance σ_g^2.

454 Accordingly, as Θ increases, so does σ_g^2 and, thus, γ (eq. 6b). In the limit $t \to \infty$, the

455 population will follow the optimum at a constant lag $\delta_{eq} = \frac{v}{\gamma}$. Thus, if v is large (such that,

456 even for large σ_g^2, the lag is large relative to the mutational standard deviation σ_m) increasing

457 Θ does not affect $\bar{\alpha}$. In contrast, if v is small, increasing Θ (and, hence, σ_g^2) will reduce the

458 lag even further, such that most large-effect alleles will be deleterious. Consequently, for

459 small v, $\bar{\alpha}$ decreases as Θ increases.

460 The width of the fitness landscape σ_s^2 affects different aspects of the adaptive process, but its

461 net effect is an increase of the mean effect size of fixed alleles as σ_s^2 increases (i.e., as stabilizing

462 selection gets weaker), especially if the rate of environmental change is intermediate (Fig. 4D).

463 The reason is that weak stabilizing selection increases the frequency of large-effect alleles in

464 the standing variation. In addition, weak selection also increases the phenotypic lag (eq. 9;

465 see also KOPP and MATUSZEWSKI 2014), again favoring large effect alleles. Note that the

466 latter point holds true even though weak selection increases the background variance σ_g^2.

467 Finally, the effect of σ_s^2 is strongest for intermediate v, because for small v, large-effect alleles

468 are never favored, whereas for large v, all alleles with positive effect have a high fixation

469 probability.

470 Similar arguments hold for N_e (when the rate of mutational supply, Θ, is held constant).

471 First, increasing N_e will always increase the efficacy of selection, resulting in lower initial

472 frequencies of mutant alleles (eq. A4) and decreased σ_g^2 (eq. 16). If the environment changes

473 slowly, $\bar{\alpha}$ increases with N_e, because the equilibrium lag increases (caused by the decrease

474 in σ_g^2). In contrast, if the rate of environmental change is fast, $\bar{\alpha}$ slightly decreases with N_e

475 due to the lower starting frequency of large-effect alleles and because small-effect alleles are

29

476 selected more efficiently (i.e., they are less prone to get lost by genetic drift; Fig. 4F).

477 The potential for adaptation from standing genetic variation and the rate of

478 environmental change

479 So far, we have focussed on the distribution of adaptive substitutions for individual fixation

480 events. We now address what can be said about the total progress that can be made from

481 standing genetic variation following a moving phenotypic optimum. The overall potential for

482 adaptation from standing genetic variation depends on the mean number of alleles segregating

483 in the standing genetic variation, which can be accurately approximated as (FOLEY 1992)

$$|\mathcal{G}| = 1 + \Theta \log \left[\frac{2\sigma_s^2}{\sigma_m^2} \right] \tag{26}$$

484 (results not shown). The mean number of alleles that become fixed can then be calculated

485 as

$$|\mathcal{G}|_{\text{fix}} = |\mathcal{G}| \int_0^{\alpha_{\max}} p(\alpha) \Pi_{\text{seg}}(\alpha) \mathrm{d}\alpha, \tag{27}$$

486 where the integral equals the normalization constant in equation (19) (i.e., the proportion of

487 fixed alleles). Finally, using equation (27), the average distance travelled in phenotype space

488 before standing variation is exhausted is given by

$$z^* = 2|\mathcal{G}|_{\text{fix}} \bar{\alpha} = 2|\mathcal{G}| \int_0^{\alpha_{\max}} \alpha p(\alpha) \Pi_{\text{seg}}(\alpha) \mathrm{d}\alpha, \tag{28}$$

489 where $\bar{\alpha}$ is the mean phenotypic effect size of adaptive substitutions from standing genetic

490 variation, and the factor 2 in equation (28) comes from the fact that we are considering

491 diploids (and α denotes the phenotypic effect per haplotype). Note that, once the shift of

492 the optimum considerably exceeds z^*, the population will inevitably go extinct without the

493 input of new mutations.

30

494 Figure 6 (see also Figs. S3_3, S3_4, S3_5 and Figs. S3_6, S3_7) illustrate these predictions

495 and compare them to results from individual-base simulations (where, unlike in the rest of

496 this paper, new mutational input was turned off after the onset of the environmental change).

497 Both the mean number of fixations $|\mathcal{G}|_{\text{fix}}$ and the mean phenotypic distance travelled z^*

498 increase with the rate of environmental change, reflecting the fact that more and larger-effect

499 alleles become fixed if the environment changes fast. Only for very large v, where the rate

500 of environmental change exceeds the "maximal sustainable rate of environmental change"

501 (Bürger and Lynch 1995), which for our choice for the number of offspring $B = 2$ equals

$$v_{\text{crit}} = \sigma_g^2 \sqrt{\frac{2\log\left[2\sqrt{\frac{\sigma_s^2}{\sigma_g^2+\sigma_s^2}}\right]}{\sigma_g^2 + \sigma_s^2}}, \tag{29}$$

502 do $|\mathcal{G}|_{\text{fix}}$ and z^* decrease sharply, because the population goes extinct before fixations can be

503 completed (grey-dashed line in Figs. 6, S3_6 and S3_7). At small values of v, $|\mathcal{G}|_{\text{fix}}$ matches

504 the "neutral" prediction (grey-dashed line in Figs. S3_3, S3_4 and S3_5). Note that these

505 fixations have almost no effect on z^*, because their average effect is zero. At intermediate

506 v, equation (28) slightly underestimates z^* for parameter values leading to large background

507 variance σ_g^2 (i.e., high Θ and σ_s^2). The likely reason is that the analytical approximation

508 assumes σ_g^2 to be constant, while it obviously decreases in the simulations (since there are

509 no *de-novo* mutations). All these results are qualitatively consistent across different values

510 of σ_s^2 and Θ (Figs. 6, S3_6, S3_7).

Figure 6 – The average distance traversed in phenotype space, z^*, as a function of the rate of environmental change v, when standing genetic variation is the sole source for adaptation. Symbols show results from individual-based simulations (averaged over 100 replicate runs). The black line gives the analytical prediction (eq. 28), with σ_g^2 taken from equation (16). The grey-dashed line gives the critical rate of environmental change (eq. 29). Error bars for standard errors are contained within the symbols. Fixed parameters: $N = 2500$, $\sigma_m^2 = 0.05$.

511
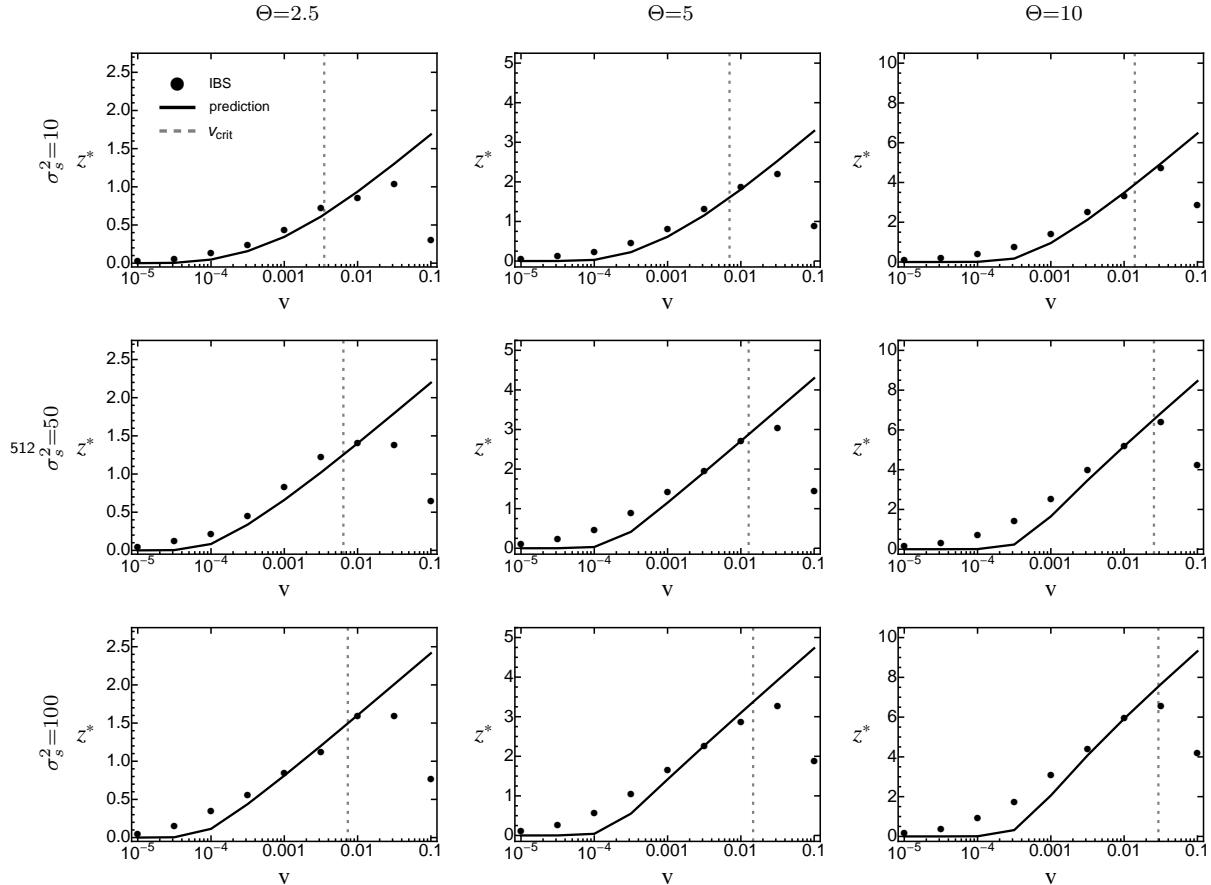
The relative importance of standing genetic variation and *de-novo* mutations over the course of adaptation

Until now we have compared adaptation from standing genetic variation to that from *de-novo* mutations in terms of their distribution of fixed phenotypic effects. We now turn to investigating their relative importance over the course of adaptation. For this purpose, we recorded (in individual-based simulations) the contributions of both sources of variation to the phenotypic mean and variance. An average time series for both measures is shown in Figure 7. As expected, the initial response to selection is almost entirely based on standing variation, but the contribution of *de-novo* mutations increases over time. As a quantitative

522 measure for this transition, we define $t_{\mathrm{DNM},50}(\bar{z})$ as the point in time where the cumulative

523 contribution of *de-novo* mutations has reached 50%. Indeed, we find that, beyond this time,

524 adaptation almost exclusively proceeds by the fixation of *de-novo* mutations (Fig. 7A). As

525 expected, $t_{\mathrm{DNM},50}(\bar{z})$ decreases with v (Figs. 8, S3_8, first row), while the total phenotypic

526 response $\bar{z}$ increases (Figs. 8, S3_8, second row). The reason is that faster environmental

527 change induces stronger directional selection and increases the phenotypic lag, such that

528 standing variation is depleted more quickly and *de-novo* mutations and contribute earlier.

529 Note that, as in Figure 6, the total phenotypic response at time $t_{\mathrm{DNM},50}(\bar{z})$ decreases once

530 v exceeds the "maximal sustainable rate of environmental change", for the same reasons as

531 discussed above. Furthermore, $t_{\mathrm{DNM},50}(\bar{z})$ increases with both Θ and σ_s^2 (due to the increased

532 standing variation; see eq. 16). Interestingly, the relative contribution of original standing

533 genetic variation to the total genetic variance at time $t_{\mathrm{DNM},50}(\bar{z})$ remains largely constant (at

534 around 20%) over large range of v and does not show any dependence on Θ nor σ_s^2 (Figs. 8,

535 S3_8; third row). Deviations occur only if v is either very small or very large. In particular,

536 if v is small, standing variation is almost completely depleted before new mutations play

537 a significant role. Conversely, if v is very large, standing genetic variation still forms the

538 majority of the total genetic variance. As mentioned above, this is most likely because the

539 population goes extinct before fixations can be completed, that is, before the entire (standing)

540 adaptive potential is exhausted. All these results remain qualitatively unchanged if, instead

541 of $t_{\mathrm{DNM},50}(\bar{z})$, we define $t_{\mathrm{DNM},50}(\sigma_g^2)$ as the point in time where 50% of the current genetic

542 variance goes back to *de-novo* mutations (Figs. S3_9, S3_10).
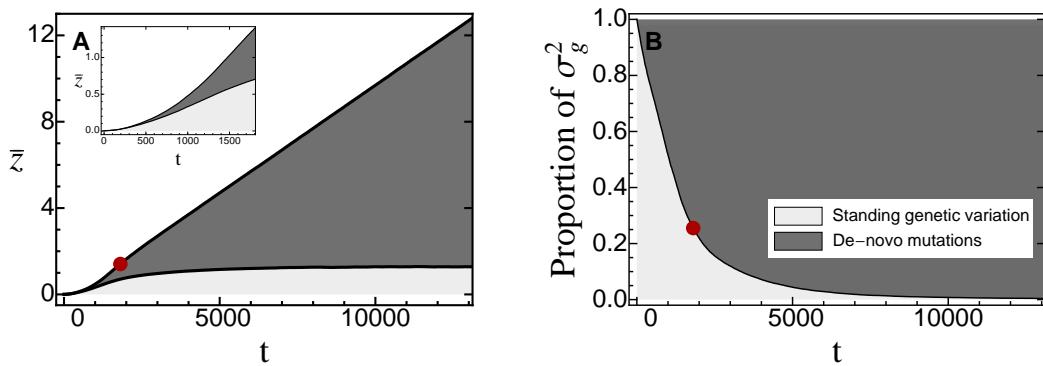
Figure 7 – The contributions of standing genetic variation (light grey) and *de-novo* mutations (dark grey) to the cumulative phenotypic response to selection $\bar{z}$ (A) and the *current* genetic variance (B) over time. Plots show average trajectories over 1000 replicate simulations. The red dot marks the point in time where 50% of the total phenotypic response were due to *de-novo* mutations. The inset in (A) shows a more detailed plot of the dynamics of $\bar{z}$ up to this point. Fixed parameters: $\sigma_s^2 = 50$, $\Theta = 5$, $N = 2500$, $v = 0.001$, $\sigma_m^2 = 0.05$.
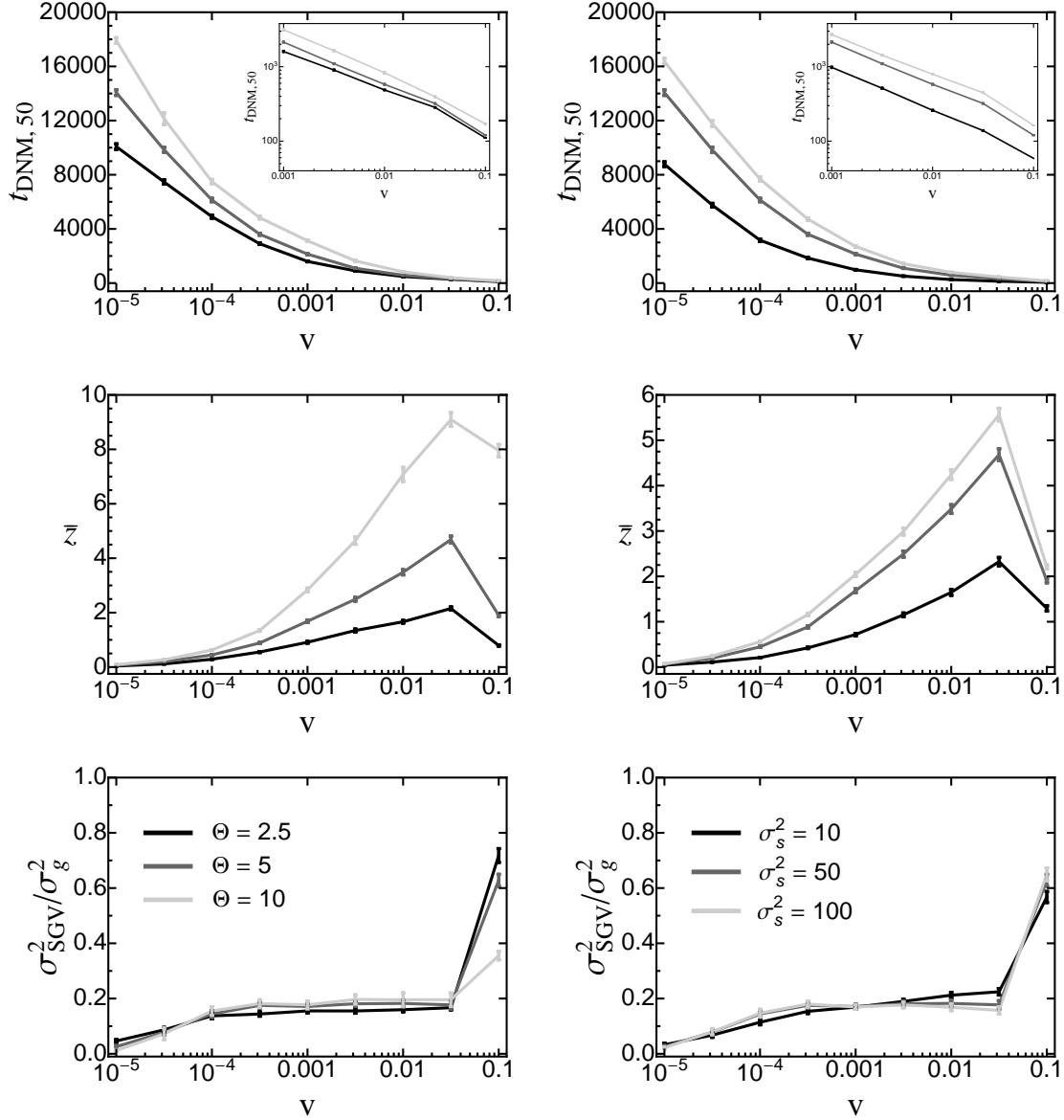
Figure 8 – First row: the point in time $t_{\mathrm{DNM},50}$ ($\bar{z}$) where 50% of the phenotypic response to moving-optimum selection have been contributed by *de-novo* mutations as a function of the rate of environmental change for various values of Θ (left) and σ_s^2 (right). Insets show the results for large v on a log-scale. Second row: The mean total phenotypic response at this time. Third row: The relative contribution of original standing genetic variation to the total genetic variance at time $t_{\mathrm{DNM},50}$ ($\bar{z}$). Data are means (and standard deviations) from 1000 replicate simulation runs. Fixed parameters (if not stated otherwise): $\sigma_s^2 = 50$, $\Theta = 5$, $N = 2500$, $\sigma_m^2 = 0.05$.

35

DISCUSSION

Global climate change has forced many populations to either go extinct or adapt to the altered environmental condition. When studying the genetic basis of this process, most theoretical work has focused on adaptation from new mutations (e.g., GILLESPIE 1984; ORR 1998, 2000; COLLINS *et al.* 2007; KOPP and HERMISSON 2007, 2009a,b; MATUSZEWSKI *et al.* 2014). Consequently, very little is known about the details of adaptation from standing genetic variation (but see ORR and BETANCOURT 2001; HERMISSON and PENNINGS 2005), that is, which of the alleles segregating in a population will become fixed and contribute to the evolutionary response. Here, we have used analytical approximations and stochastic simulations to study the effects of standing genetic variation on the genetic basis of adaptation in gradually changing environments. Supporting a verbal hypothesis by BARRETT and SCHLUTER (2008), we show that, when comparing adaptation from standing genetic variation to that from *de-novo* mutations, the former proceeds, on average, by the fixation of more alleles of small effect. In both cases, however, the genetic basis of adaptation crucially depends on the efficacy of selection, which in turn is determined by the population size, the strength of (stabilizing) selection and the rate of environmental change. When standing genetic variation is the sole source for adaptation, we find that fast environmental change enables the population to traverse larger distances in phenotype space than slow environmental change, in contrast to studies that consider adaptation from new mutations only (PERRON *et al.* 2008; BELL and GONZALEZ 2011; LINDSEY *et al.* 2013; BELL 2013). We now discuss these results in greater detail.

The genetic basis of adaptation in the moving-optimum model

Introduced as a model for sustained environmental change, such as global warming (LYNCH *et al.* 1991; LYNCH and LANDE 1993), the moving-optimum model describes the evolution of a quantitative trait under stabilizing selection towards a time-dependent optimum (BÜRGER 2000). A large number of studies have analyzed both the basic model and several modifi-

568 cations, for example, models with a periodic or fluctuating optimum, or models for multi-

569 ple traits (SLATKIN and LANDE 1976; CHARLESWORTH 1993; BÜRGER and LYNCH 1995;

570 LANDE and SHANNON 1996; KOPP and HERMISSON 2007, 2009a,b; GOMULKIEWICZ and

571 HOULE 2009; ZHANG 2012; CHEVIN 2013; MATUSZEWSKI *et al.* 2014). Following traditional

572 quantitative-genetic approaches, the majority of these studies assumed that the distribution

573 of genotypes (and phenotypes) is Gaussian with constant (time-invariant) genetic variance,

574 and they have mostly focussed on the evolution of the population mean phenotype and on

575 the conditions for population persistence (BÜRGER and LYNCH 1995; LANDE and SHANNON

576 1996; GOMULKIEWICZ and HOULE 2009). None of these models, however, allows to address

577 the fate of individual alleles (i.e., whether they become fixed or not). In a recent series of

578 papers on the moving-optimum model, KOPP and HERMISSON (2007, 2009a,b) studied the

579 genetic basis of adaptation from new mutations and derived the distribution of adaptive

580 substitutions (i.e, the distribution of the phenotypic effects of those mutations that arise

581 and become fixed in a population); this approach has recently been generalized to multiple

582 phenotypic traits by MATUSZEWSKI *et al.* (2014). The shape of this distribution resembles

583 a Gamma-distribution with an intermediate mode. Thus, most substitutions are of inter-

584 mediate effect with only a few large-effect alleles contributing to adaptation. The reason is

585 that small-effect alleles – despite appearing more frequently than large-effect alleles – have

586 only small effects on fitness (and are, hence, often lost due to genetic drift), while large-effect

587 alleles might be removed because they "overshoot" the optimum (KOPP and HERMISSON

588 2009b). A detailed comparison and discussion of the distribution of adaptive substitutions

589 from *de-novo* mutations with (eq. 23) and without (KOPP and HERMISSON 2009b) genetic

590 background variation is given in Supporting Information 2.

591 Here, we have studied the genetic basis of adaptation from standing genetic variation. We

592 find that the distribution of substitutions from standing genetic variation depends on the

593 distribution of standing genetic variants (i.e., distribution of alleles segregating in the popu-

594 lation prior to the environmental change) and the intensity of selection. The former is shaped

37

595 primarily by the distribution of new mutations and the strength of stabilizing selection, which

596 removes large-effect alleles. Depending on the speed of change v, we find two regimes that are

597 characterized by separate distributions of standing substitutions. If the environment changes

598 sufficiently fast, the distribution of adaptive substitutions resembles a lognormal distribu-

599 tion with a strong contribution of small-effect alleles (eq. 19; Fig. 2). The reason is that, in

600 the standing genetic variation, small-effect alleles are more frequent than large-effect alleles

601 and might already segregate at appreciable frequency (so that they are not lost by genetic

602 drift). With a moving optimum, they furthermore are the first to become positively selected,

603 hence reducing the time they are under purifying selection. Finally, epistatic interactions

604 between co-segregating alleles (or between a focal allele and the genetic background) also

605 favor alleles of small effect. Consequently, when adapting from standing genetic variation,

606 most substitutions are of small phenotypic effect.

607 The second regime occurs if the rate of environmental change v is very small. In this case,

608 allele-frequency dynamics are dominated by genetic drift, and the distribution of adaptive

609 substitutions reflects the approximately Gaussian distribution of standing genetic variants

610 (eq. 25; Fig. S3_2). It should be noted, however, that fixations under this regime take a very

611 long time, similar to that of purely neutral substitutions (i.e., on the timescale of $4N_e$).

612 Finally, we have studied the relative importance of standing genetic variation and *de-novo*

613 mutations over the course of adaptation. As shown in Figures 7 and 8, the initial response

614 to selection is almost entirely based on standing variation, with *de-novo* mutations becoming

615 gradually more important. The time scale of this transition strongly depends on the rate

616 of environmental change, but for slow or moderately fast change, it typically occurs over at

617 least hundreds of generations (Figs. 8, S3_8 and Figs. S3_9, S3_10). This observation is

618 in contrast to results by HILL and RASBASH (1986b), who found that under strong artificial

619 (i.e., truncation) selection in small populations ($N = 20$), new mutations might contribute

620 up to one third of the total response after as little as 20 generations. Our results show

621 that the situation is very different for large populations under natural selection in gradually

38

changing environments. The likely reason for this difference is that truncation selection induces strong directional selection (corresponding to large v) and only extreme phenotypes reproduce. Thus, truncation selection is much more efficient in maintaining large-effect *de-novo* mutations, while eroding genetic variation more quickly (because it introduces a large skew in the offspring distribution). However, the similarities and differences in the genetic basis of responses to artificial versus natural selection is an interesting topic—in particular, for the interpretation of the large amount of genetic data available from breeding programs (STERN and ORGONZO 2009)—that should be addressed in future studies.

Throughout this study, we have focused on adaptation to a moving optimum, that is, a scenario of gradual environmental change. An obvious question is how our results would change under the alternative scenario of a one-time sudden shift in the optimum (as assumed in numerous studies, e.g., ORR 1998; HERMISSON and PENNINGS 2005; CHEVIN and HOSPITAL 2008). While beyond the scope of this paper, our approach should, in principle, still be applicable. In particular, each focal allele still experiences a gradual change in its selection coefficient, due to the evolution of the genetic background. Unlike in the moving-optimum model, however, the selection coefficient *decreases*, as the mean phenotype gradually approaches the new optimum. Hence, a suitably modified version of equation 13 would give the probability that a focal allele *establishes* in the population (i.e., escapes stochastic loss), but in the absence of continued environmental change, establishment does not guarantee fixation. In other words, alleles need to "race for fixation" before other competing alleles get fixed and they become deleterious (KOPP and HERMISSON 2007, 2009a). The dynamics of a mutation along its trajectory should therefore be even more complex than in the moving-optimum model, and show an even stronger dependence on the genetic background (CHEVIN and HOSPITAL 2008).

Extinction and the rate of environmental change

Recently, several experimental studies have explored how the rate of environmental change

39

648 affects the persistence of populations that rely on new mutations for adapting to a gradually

649 changing environment (PERRON *et al.* 2008; BELL and GONZALEZ 2011; LINDSEY *et al.*

650 2013). In line with theoretical predictions (BELL 2013), all studies found that "evolutionary

651 rescue" is contingent on a small rate of environmental change. In particular, LINDSEY *et al.*

652 (2013) evolved replicate populations of *E. coli* under different rates of increase in antibiotic

653 concentration and found that certain genotypes were evolutionarily inaccessible under rapid

654 environmental change, suggesting that "rapidly deteriorating environments not only limit

655 mutational opportunities by lowering population size, but [...] also eliminate sets of mutations

656 as evolutionary options". This is in stark contrast to our prediction that faster environmental

657 change can enable the population to remain better adapted and to traverse larger distances

658 in phenotype space when standing genetic variation is the sole source for adaptation (Fig. 6

659 and Figs S3_6, S3_7; in line with recent experimental observations; H. Teotonio, private

660 communication). The difference between these results arises from the availability of the

661 "adaptive material". While *de-novo* mutations first need to appear and survive stochastic loss

662 before becoming fixed, standing genetic variants are available right away and might already

663 be segregating at appreciable frequency. Thus, in both cases, the rate of environmental

664 change plays a critical, though antagonistic, role in determining the evolutionary options.

665 While fast environmental change eliminates sets of new mutations, it simultaneously helps

666 to preserve standing genetic variation until it can be picked-up by selection. Under slow

667 change, in contrast, most large-effect alleles from the standing variation, by the time they

668 are needed, are already eliminated by drift or stabilizing selection.

669 Our results also mean that, if the optimum stops moving at a given value $z_{\mathrm{opt,max}}$, popula-

670 tions will achieve a higher degree of adaptation (higher $\bar{z}^*$) if the final optimum is reached

671 fast rather than slowly (see also UECKER and HERMISSON 2014), at least if standing genetic

672 variation is the sole source for adaptation. While this assumption is an obvious simplification,

673 it may often be approximately true in natural populations. The same holds true in exper-

674 imental populations, where selection is usually strong and the duration of the experiment

40

675 short, such that *de-novo* mutations can frequently be neglected (see Fig. 8).

Testing the predictions

677 The predictions made by our model can in principle be tested empirically, even though suit-
678 able data might be sparse and experiments challenging. There is, of course, ample evidence
679 for adaptation from standing genetic variation. For example, DOMINGUES *et al.* (2012)
680 showed that camouflaging pigmentation of oldfield mice (*Peromyscus polionotus*) that have
681 colonized Florida's Gulf Coast has evolved quite rapidly from a pre-existing mutation in the
682 *Mc1r* gene; LIMBORG *et al.* (2014) investigated selection in two allochronic but sympatric
683 lineages of pink salmon (*Oncorhynchus gorbuscha*) and identified 24 divergent loci that had
684 arisen from different pools of standing genetic variation, and TURCHIN *et al.* (2012) showed
685 that height-associated alleles in humans display a clear signal for widespread selection on
686 standing genetic variation.

687 However, testing the predictions of our model requires, in addition, detailed knowledge of
688 the genotype-phenotype relation. Currently, there is only a small (yet increasing) number of
689 systems for which both a set of functionally validated beneficial mutations and their selec-
690 tion coefficients under different environmental conditions are available (JENSEN 2014). Thus,
691 estimating the distribution of standing substitutions will be challenging, because of the of-
692 ten unknown phenotypic and fitness effects of beneficial mutations and the large number of
693 replicate experiments needed to obtain a reliable empirical distribution. Furthermore, even if
694 these problems were solved, small-effect alleles might not be detectable due to statistical lim-
695 itations (OTTO and JONES 2000), and in certain limiting cases where the population quickly
696 goes extinct (i.e., when the environment changes very fast), the distribution of adaptive sub-
697 stitutions from standing genetic variation might be indistinguishable to that from *de-novo*
698 substitutions (Fig. 5).

699 Recent developments in laboratory systems (MORRAN *et al.* 2009; PARTS *et al.* 2011), how-
700 ever, have created opportunities for experimental evolution studies in which population size,

41

the selective regime and the duration of selection can be manipulated, and adaptation from *de-novo* mutations and standing genetic variation can be recorded (Burke 2012). Applying these techniques in experiments in the vein of Lindsey *et al.* (2013), but starting from a polymorphic population, should make it possible to test the relation between the rate of environmental change and population persistence, and to assess the probability of adaptation from standing genetic variation. First experiments along these lines are currently being carried out in populations of *C. elegans*, with the aim of determining the limits of adaptation to different rates of increase in sodium chloride concentration (H. Teotonio, private communication). Furthermore, Pennings (2012) recently applied the Hermisson and Pennings (2005) framework to show that standing genetic variation plays an important role in the evolution of drug-resistance in *HIV*, affecting up to 39% of patients (depending on treatment) and explaining why resistance mutations in patients who interrupt treatment are likely to become established within the first year. A similar approach should also be applicable to scenarios of gradual environmental change (e.g., evolution of resistance mutations under gradually increasing antibiotic concentrations).

Conclusion

As global climate change continues to force populations to respond to the altered environmental conditions, studying adaptation to changing environments – both empirically and theoretically – has become one of the main topics in evolutionary biology. Despite increased efforts, however, very little is known about the genetic basis of adaptation from standing genetic variation. Our analysis of the moving-optimum model shows that this process has, indeed, a very different genetic basis than that of adaptation from *de-novo* mutations. In particular, adaptation proceeds via the fixation many small-effect alleles (and just a few large ones). In accordance with previous studies, the adaptive process critically depends on the tempo of environmental change. Specifically, when populations adapt from standing genetic variation only, the potential for adaptation increases as the environment changes faster.

42

Acknowledgements

LITERATURE CITED

BARRETT, R. D., and D. SCHLUTER, 2008 Adaptation from standing genetic variation. Trends Ecol. Evol. **23**: 38–44.

BARTON, N. H., and M. TURELLI, 1991 Natural and sexual selection on many loci. Genetics **127**: 229–55.

BELL, G., 2009 The oligogenic view of adaptation. Cold Spring Harbor Symposia on Quantitative Biology **74**: 139–144.

BELL, G., 2013 Evolutionary rescue and the limits of adaptation. Philos. Tr. R. Soc. Lon. B **368**: 20120080.

BELL, G., and A. GONZALEZ, 2011 Adaptation and evolutionary rescue in metapopulations experiencing environmental deterioration. Science **332**: 1327–1330.

BULMER, M. G., 1980 *The mathematical theory of quantitative genetics*. Oxford University Press, Oxford.

BÜRGER, R., 2000 *The mathematical theory of selection, recombination, and mutation*. Wiley, Chichester.

BÜRGER, R., and M. LYNCH, 1995 Evolution and extinction in a changing environment: a quantitative genetic analysis. Evolution **49**: 151–163.

BURKE, M. K., 2012 How does adaptation sweep through the genome? Insights from long-term selection experiments. Proc. R. Soc. B **279**: 5029–5038.

CAPRIO, M., 2005 Levelscheme: A level scheme drawing and scientific figure preparation system for mathematica. Comput. Phys. Commun. **171**: 107 – 118.

CHARLESWORTH, B., 1993 Directional selection and the evolution of sex and recombination. Genetical Research Cambridge **61**: 205–224.

CHEVIN, L. M., 2013 Genetic constraints on adaptation to a changing environment. Evolution **67**: 708–721.

CHEVIN, L. M., and F. HOSPITAL, 2008 Selective sweep at a quantitative trait locus in the presence of background genetic variation. Genetics **180**: 1645–1660.

44

COLLINS, S., J. DE MEAUX, and C. ACQUISTI, 2007 Adaptive walks toward a moving optimum. Genetics **176**: 1089–1099.

COMERON, J. M., A. WILLIFORD, and R. M. KLIMAN, 2008 The Hill-Robertson effect: evolutionary consequences of weak selection and linkage in finite populations. Heredity **100**: 19–31.

COOPER, T. F., E. A. OSTROWSKI, and M. TRAVISANO, 2007 A negative relationship between mutation pleiotropy and fitness effect in yeast. Evolution **61**: 1495–1499.

DOMINGUES, V. S., Y.-P. POH, B. K. PETERSON, P. S. PENNINGS, J. D. JENSEN, *et al.*, 2012 Evidence of adaptation from ancestral variation in young populations of beach mice. Evolution **66**: 3209–3223.

EWENS, W. J., 2004 *Mathematical population genetics.* Springer-Verlag, Berlin, 2nd edition.

FOLEY, P., 1992 Small Population Genetic Variability at Loci Under Stabilizing Selection. Evolution **46**: 763–774.

GALASSI, M., J. DAVIES, J. THEILER, B. GOUGH, and G. JUNGMAN, 2009 *GNU Scientific Library - Reference Manual, Third Edition, for GSL Version 1.12 (3. ed.)..* Network Theory Ltd.

GILLESPIE, J. H., 1984 Molecular evolution over the mutational landscape. Evolution **38**: 1116–1129.

GOMULKIEWICZ, R., R. D. HOLT, M. BARFIELD, and S. L. NUISMER, 2010 Genetics, adaptation, and invasion in harsh environments. Evol. Appl. **3**: 97–108.

GOMULKIEWICZ, R., and D. HOULE, 2009 Demographic and genetic constraints on evolution. Am. Nat. **174**: E218–229.

HALLAUER, A., M. CARENA, and J. FILHO, 2010 *Quantitative Genetics in Maize Breeding.* Handbook of Plant Breeding. Springer.

HERMISSON, J., and P. S. PENNINGS, 2005 Soft sweeps: molecular population genetics of adaptation from standing genetic variation. Genetics **169**: 2335–2352.

HIETPAS, R. T., C. BANK, J. D. JENSEN, and D. N. A. BOLON, 2013 Shifting fitness

45

787   landscapes in response to altered environments. Evolution **67**: 3512–3522.

788 HILL, W. G., and J. RASBASH, 1986a Models of long-term artificial selection in finite

789   population. Genet. Res. **48**: 41–50.

790 HILL, W. G., and J. RASBASH, 1986b Models of long-term artificial selection in finite

791   population with recurrent mutation. Genet. Res. **48**: 125–131.

792 HILL, W. G., and A. ROBERTSON, 1966 The effect of linkage on limits to artificial selection.

793   Genet. Res. **8**: 269–294.

794 JENSEN, J. D., 2014 On the unfounded enthusiasm for soft selective sweeps. Nat. Commun.

795   **5**: 5281.

796 JONES, A. G., S. J. ARNOLD, and R. BÜRGER, 2004 Evolution and stability of the G-matrix

797   on a landscape with a moving optimum. Evolution **58**: 1636–1654.

798 JONES, A. G., R. BÜRGER, S. J. ARNOLD, P. A. HOHENLOHE, and J. C. UYEDA, 2012

799   The effects of stochastic and episodic movement of the optimum on the evolution of the

800   G-matrix and the response of the trait mean to selection. J. Evol. Biol. **25**: 2010–2031.

801 KAUFFMAN, S. A. A., and S. LEVIN, 1987 Towards a general theory of adaptive walks on

802   rugged landscapes. J. Theor. Biol. **128**: 11–45.

803 KIMURA, M., 1957 Some problems of stochastic processes in genetics. Ann. Math. Stat. **28**:

804   882–901.

805 KIMURA, M., 1983 *The neutral theory of molecular evolution*. Cambridge University Press,

806   Cambridge.

807 KIRKPATRICK, M., T. JOHNSON, and N. BARTON, 2002 General models of multilocus

808   evolution. Genetics **161**: 1727–1750.

809 KOPP, M., and J. HERMISSON, 2007 Adaptation of a quantitative trait to a moving optimum.

810   Genetics **176**: 715–718.

811 KOPP, M., and J. HERMISSON, 2009a The genetic basis of phenotypic adaptation I: Fixation

812   of beneficial mutations in the moving optimum model. Genetics **182**: 233–249.

813 KOPP, M., and J. HERMISSON, 2009b The genetic basis of phenotypic adaptation II: The

distribution of adaptive substitutions in the moving optimum model. Genetics **183**: 1453–1476.

KOPP, M., and S. MATUSZEWSKI, 2014 Rapid evolution of quantitative traits: theoretical perspectives. Evol. Appl. **7**: 169–191.

LANDE, R., 1976 The maintenance of genetic variability by mutation in a polygenic character with linked loci. Genet. Res. **26**: 221–235.

LANDE, R., 1983 The response to selection on major and minor mutations affecting a metrical trait. Heredity **50**: 47–65.

LANDE, R., and S. SHANNON, 1996 The role of genetic variation in adaptation and population persistence changing environment. Evolution **50**: 434–437.

LANG, G. I., D. BOTSTEIN, and M. M. DESAI, 2011 Genetic variation and the fate of beneficial mutations in asexual populations. Genetics **188**: 647–661.

LIMBORG, M. T., R. K. WAPLES, J. E. SEEB, and L. W. SEEB, 2014 Temporally isolated lineages of pink salmon reveal unique signatures of selection on distinct pools of standing genetic variation. Heredity **105**: 741–751.

LINDSEY, H. A., J. GALLIE, S. TAYLOR, and B. KERR, 2013 Evolutionary rescue from extinction is contingent on a lower rate of environmental change. Nature **494**: 463–467.

LYNCH, M., W. GABRIEL, and A. M. WOOD, 1991 Adaptive and demographic responses of plankton populations to environmental change. Limnol. Oceanogr. **36**: 1301–1312.

LYNCH, M., and R. LANDE, 1993 Evolution and extinction in response to environmental change. In P. Kareiva, J. G. Kingsolver and R. B. Juey, editors, *Biotic interactions and global change.* Sinauer, Sunderland, 43–53.

MARTIN, G., and T. LENORMAND, 2006a A general multivariate extension of Fisher's geometrical model and the distribution of mutation fitness effects across species. Evolution **60**: 893–907.

MARTIN, G., and T. LENORMAND, 2006b The fitness effect of mutations in stressful environments: a survey in the light of fitness landscape models. Evolution **60**: 2413–2427.

47

MATUSZEWSKI, S., J. HERMISSON, and M. KOPP, 2014 Fisher's geometric model with a moving optimum. Evolution **68**: 2571–2588.

MORRAN, L. T., M. D. PARMENTER, and P. C. PHILLIPS, 2009 Mutation load and rapid adaptation favour outcrossing over self-fertilization. Nature **462**: 350–352.

ORR, H. A., 1998 The population genetics of adaptation: the distribution of factors fixed during adaptive evolution. Evolution **52**: 935–949.

ORR, H. A., 2000 Adaptation and the cost of complexity. Evolution **54**: 13–20.

ORR, H. A., 2002 The population genetics of adaptation: the adaptation of DNA sequences. Evolution **56**: 1317–1330.

ORR, H. A., 2005a The genetic theory of adaptation: a brief history. Nat. Rev. Gen. **6**: 119–127.

ORR, H. A., 2005b Theories of adaptation: what they do and don't say. Genetica **123**: 3–13.

ORR, H. A., and A. J. BETANCOURT, 2001 Haldane's sieve and adaptation from standing genetic variation. Genetics **157**: 875–884.

OTTO, S. P., and C. D. JONES, 2000 Detecting the undetected: estimating the total number of loci underlying a quantitative trait. Genetics **156**: 2093–2107.

PARTS, L., F. A. CUBILLOS, J. WARRINGER, K. JAIN, F. SALINAS, *et al.*, 2011 Revealing the genetic structure of a trait by sequencing a population under selection. Genome Res. **21**: 1131–1138.

PENNINGS, P. S., 2012 Standing genetic variation and the evolution of drug resistance in HIV. PLoS Comput. Biol. **8**: e1002527.

PERRON, G. G., A. GONZALEZ, and A. BUCKLING, 2008 The rate of environmental change drives adaptation to an antibiotic sink. J. Evol. Biol. **21**: 1724–1731.

ROCKMAN, M. V., 2012 The QTN program and the alleles that matter for evolution: all that's gold does not glitter. Evolution **66**: 1–17.

SLATKIN, M., and R. LANDE, 1976 Niche width in a fluctuating environment-density inde-

pendent model. Am. Nat. **110**: pp. 31–55.

SMITH, N. G. C., and A. EYRE-WALKER, 2002 Adaptive protein evolution in Drosophila. N **415**: 1022–1024.

SPEED, T. P., 2005 *Genetic Map Functions*. John Wiley & Sons, Ltd, 2nd edition.

STERN, D. L., and V. ORGONZO, 2009 Is genetic evolution predictable? Science **323**: 746–751.

TOBIN, D., A. KAUSE, E. A. MÄNTYSAARI, S. A. MARTIN, D. F. HOULIHAN, *et al.*, 2006 Fat or lean? The quantitative genetic basis for selection strategies of muscle and body composition traits in breeding schemes of rainbow trout (*Oncorhynchus mykiss*). Aquaculture **261**: 510–521.

TURCHIN, M. C., C. W. CHIANG, C. D. PALMER, S. SANKARARAMAN, D. REICH, *et al.*, 2012 Evidence of widespread selection on standing variation in europe at height-associated snps. Nat. Gen. **44**: 1015–1019.

UECKER, H., and J. HERMISSON, 2011 On the fixation process of a beneficial mutation in a variable environment. Genetics **188**: 915–930.

UECKER, H. OTTO, S. P., and J. HERMISSON, 2014 Evolutionary rescue in structued populations. Am. Nat. **183**: E17–E35.

WICHMAN, H. A., M. R. BADGETT, L. A. SCOTT, C. M. BOULIANNE, and J. J. BULL, 1999 Different trajectories of parallel evolution during viral adaptation. Science **285**: 422–424.

WRICKE, G., and E. WEBER, 1986 *Quantitative genetics and selection in plant breeding*. Walter de Gruyter.

ZHANG, X. S., 2012 Fisher's geometrical model of fitness landscape and variance in fitness within a changing environment. Evolution **66**: 2350–2368.

APPENDIX

Appendix 1: Theoretical Background

In this Appendix, we briefly recapitulate results from previous studies that form the basis for our analytical derivations.

The probability of adaptation from standing genetic variation for a single bi-allelic locus after a sudden environmental change

HERMISSON and PENNINGS (2005) studied the situation where the selection scheme at a single bi-allelic locus changes following a sudden environmental change. In particular, they derived the probability for a mutant allele to reach fixation that was neutral or deleterious prior to the change but has become beneficial in the new environment. In the continuum limit for allele frequencies this probability is given by

$$P_{\text{SGV}} = \int_0^1 \rho(x)\Pi_x \mathrm{d}x, \tag{A1}$$

where $\rho(x)$ is the density function for the allele frequency x of the mutant allele in mutation-selection-drift balance and Π_x denotes its fixation probability.

For a mutant allele present at frequency x and with selective advantage s_b in the new environment, the fixation probability is given by (KIMURA 1957)

$$\Pi_x(s_b) \approx \frac{1 - \exp[-4N_e s_b x]}{1 - \exp[-4N_e s_b]}. \tag{A2}$$

There are two points to make here. First, mutational effects in the HERMISSON and PENNINGS (2005) model are directly proportional to fitness, whereas mutations in our model affect a phenotype under selection. Second, in our framework, s_b denotes the (beneficial)

50

909   selection coefficient for heterozygotes.

910   Approximations for $\rho(x)$ can be derived from standard diffusion theory (EWENS 2004; for

911   details see HERMISSON and PENNINGS 2005). If the mutant allele was neutral prior to the

912   change in the selection scheme

$$\rho(x) = Cx^{\Theta-1}\frac{1 - x^{1-\theta}}{x - 1}. \tag{A3}$$

913   Here, $C = (\gamma + \psi(\theta))^{-1}$ denotes a normalization constant where $\gamma \approx 0.577$ is Euler's gamma

914   and $\psi(\cdot)$ is the polygamma function. Similarly, if the mutant allele was deleterious before the

915   environmental change (with negative selection coefficient s_d) the allele-frequency distribution

916   is given by

$$\rho(x) = C\frac{(1 - \exp\left[(1 - x)4N_e|s_d|\right])x^{\theta-1}}{x - 1}, \tag{A4}$$

917   where $C = ({}_1F_1(0, \theta, 4N_e|s_d|))^{-1}$ denotes a normalization constant and ${}_1F_1(a, b, c)$ is the hy-

918   pergeometric function. If the allele was sufficiently deleterious ($4N_e|s_d| \geq 10$), equation (A4)

919   can further be approximated as

$$\rho(x) = Cx^{\theta-1}\exp[-4N_e|s_d|x], \tag{A5}$$

920   where $C = (\frac{\gamma[\theta,4N_e|s_d|]}{(4N_e|s_d|)^\theta})^{-1}$ again denotes a normalization constant with $\gamma[a, b] = \int_0^b t^{a-1}\exp[-t]\mathrm{d}t$

921   denoting the lower incomplete gamma function.

922   Finally, the probability that a population successfully adapts from standing genetic variation

923   can be derived as

51

$$P_{\text{SGV}} = 1 - \left(1 + \frac{4N_e s_b}{4N_e|s_d|+1}\right)^{-\theta}$$

$$= 1 - \exp\left[-\theta \log\left[\frac{4N_e s_b}{4N_e|s_d|+1}\right]\right]. \tag{A6}$$

Fixation probabilities under time-inhomogeneous selection

In gradually changing environments, the selection coefficient of a given (mutant) allele is not fixed but changes over time (i.e., as the position of the optimum changes). UECKER and HERMISSON (2011) recently developed a mathematical framework based on branching-process theory to describe the fixation process of a beneficial allele under temporal variation in population size and selection pressures. They showed that the probability of fixation of a mutation starting with n initial copies is given by

$$\Pi_{\text{fix}}(n) = 1 - \left(1 - \frac{1}{\varphi}\right)^n, \tag{A7a}$$

where

$$2\varphi = 1 + \int_0^\infty (N(0)/N_e(t)) \exp\left[-\int_0^t s(\tau)d\tau\right] \mathrm{d}t. \tag{A7b}$$

Assuming that the population size remains constant and that the selection coefficient increases linearly in time, $s(t) = s_d + s_v t$, equation (A7a) becomes

$$\Pi_{\text{fix}} = 1 - \left(1 - \left[1 + \frac{1}{2}\sqrt{\frac{\pi}{2s_v}} \exp\left(\frac{s_d^2}{2s_v}\right) \text{erfc}\left(\frac{s_d}{\sqrt{2s_v}}\right)\right]^{-1}\right)^n, \tag{A8}$$

where $\text{erfc}(\cdot)$ denotes the complementary Gaussian error function.

SUPPORTING INFORMATION

Supporting Information 1: Limited Recombination

937

Figure S1__**1** – The distribution of adaptive substitutions from standing genetic variation for free recombination (dark bins) compared to that for limited recombination (light bins). The black line corresponds to the analytical prediction (eq. 19). σ_g^2 is given by equation (16). Fixed parameters: $\sigma_s^2 = 50$, $N = 2500$, $v = 0.001$, $\sigma_m^2 = 0.05$.

938
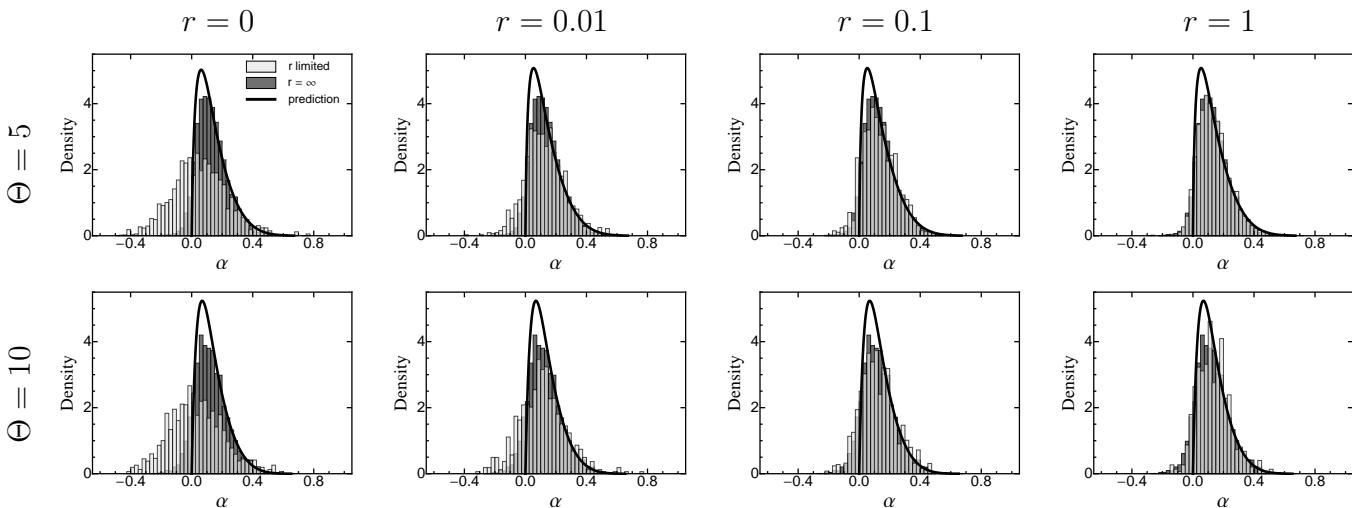
Figure S1__**2** – The distribution of adaptive substitutions from standing genetic variation for free recombination (dark bins) compared to that for limited recombination (light bins). The black line corresponds to the analytical prediction (eq. 19). σ_g^2 is given by equation (16). Fixed parameters: $\Theta = 5$, $N = 2500$, $v = 0.001$, $\sigma_m^2 = 0.05$.
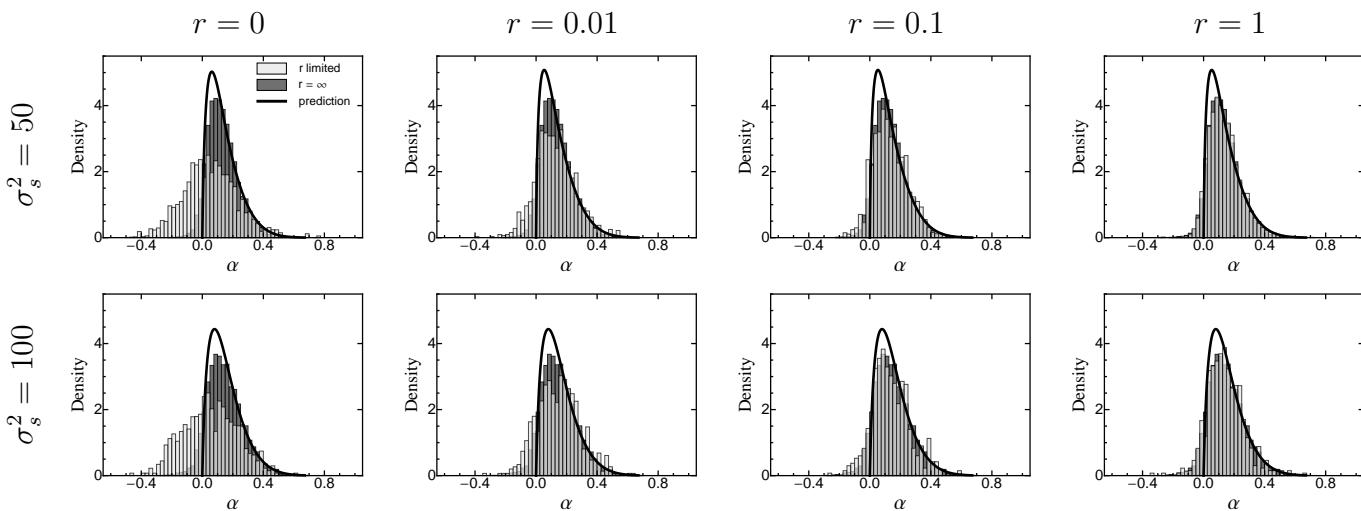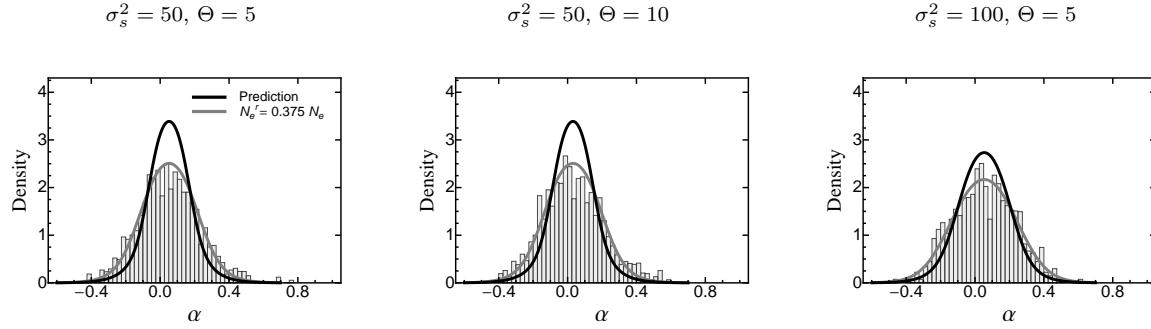
Figure S1__3 – The distribution of adaptive substitutions from standing genetic variation for complete linkage (no recombination). The black and the grey line corresponds to the analytical prediction (eq. 25) that are centred around the mean of the individual-based simulation. For the grey line N_e has been adjusted by a factor 0.385 to match the distribution from the individual-based simulations. Other parameters: $v = 0.001$, $r = 0$, $N = 2500$, $\sigma_m^2 = 0.05$.

The individual-based simulation results presented in the main text were obtained under the assumption of free recombination. In this Supplementary Information, we relax this assumption and study the effects of linkage (i.e., limited recombination).

We first clarify the meaning of the recombination parameter r, which determines the mean number of crossover events per meiosis. By definition, the simulated genome corresponds to a single chromosome of length $D_{\mathcal{G}} = r \cdot 100$cM, and the mean distance between two randomly chosen sites is $\frac{1}{3} D_{\mathcal{G}}$. The mean distance between two adjacent polymorphic loci is $D_{\mathcal{G},\text{adjacent}} = \frac{1}{|\mathcal{G}|} D_{\mathcal{G}+1}$, where $\mathcal{G}$ is the mean number of polymorphic loci, which depends on Θ and σ_s^2 (eq. 26).

The corresponding recombination rate $\mathfrak{r}$ between two polymorphic loci is given by the inverse of Haldane's mapping function (SPEED 2005), that is,

$$\mathfrak{r} = \frac{1}{2} \left(1 - \exp\left[-2 D_{\mathcal{G}} \right] \right), \tag{S1}$$

see Table S1__1.

Table S1__1 – The classical population genetic recombination rate $\mathfrak{r}$ (eq. S1) between two adjacent loci for different values of σ_s^2, Θ and r. Other parameters: $\sigma_m^2 = 0.05$.

		r			
		0	0.01	0.1	1
(Θ, σ_s^2)	$(5/50)$	0	0.019	0.16	0.49
	$(10/50)$	0	0.01	0.089	0.43
	$(5/100)$	0	0.017	0.15	0.49

The effect of limited recombination on the distribution of adaptive substitutions from standing genetic variation is illustrated in Figures S1__1 and S1__2. For $r = 1$ (corresponding to a genome length of 100cM and an average recombination rate $\mathfrak{r}$ of close to 0.5, see table S1__1), the distribution is essentially identical to that for linkage equilibrium. As r decreases, the distribution progressively shifts to the left, becomes more symmetric and includes more and more alleles with negative phenotypic effect. For $r = 0$ (corresponding to complete linkage or asexual reproduction), it resembles the distribution for "drift-driven" evolution (i.e., when selection is not efficient; Fig. S3__2). The reason is that fixation involves entire haplotypes carrying multiple mutations, whose (positive and negative) effects largely cancel. From a different perspective, limited recombination leads to Hill-Robertson interference between co-segregating alleles (HILL and ROBERTSON 1966), which in many respects corresponds to a decrease in effective population size N_e (COMERON *et al.* 2008), which in turn reduces the efficacy of selection. Note, however, that unlike in the case of a slowly changing environment (Fig. S3__2) reducing N_e also affects the equilibrium allele-frequency distribution $\rho(x, \alpha)$ (by reducing the strength of selection against large-effect alleles). In line with previous simulation results (COMERON *et al.* 2008), we find that equation (25) provides a very good fit, when N_e is set to 38.5% of its original value.

Supporting Information 2: The distribution of adaptive substitutions from *de-novo* mutations with and without genetic background variation

There are two ways in which the distribution of adaptive substitutions from standing genetic variation can be compared to that from *de-novo* mutations. The first comparison considers a population without genetic background variation. This is the situation studied by Kopp and Hermisson (2009a), where an essentially monomorphic population performs an adaptive walk following a moving optimum. The second situation is the one described by equation (23), where new mutations interact with a genetic background of constant variance (this background is presumably itself constantly replenished by new mutations). Analytical predictions for all three distributions are compared in Figures. S2_1, S2_2 and S2_3. It can be seen that the adaptive-walk prediction (eq. 14 in Kopp and Hermisson 2009b; red line) is always shifted towards larger α compared to the distribution of adaptive substitutions from standing genetic variation (eq. 19, black line). The predicted distribution from *de-novo* mutations in the presence of genetic background variation (eq. 23, grey curve) shifts from the latter to the former as v increases. The reason is that, for small v, the fixation of both standing variants and new mutations in the presence of background variation is strongly constrained by the equilibrium lag (eq. 9). For large v, in contrast, the lag is large and adaptation is primarily limited by the available alleles, independent of their source and initial frequency (mutation-limited regime *sensu* Kopp and Hermisson 2009b). Note, however, that in both limiting cases, equation (19) is a poor predictor for the simulated substitutions from standing variation (Fig. 5, S3_2). Nevertheless, it remains true that adaptive substitutions from new mutations are generally smaller than those from new mutations, with or without genetic background variation.

57

Figure S2_1 – Comparison of the analytical predictions for the distribution of adaptive substitutions from standing genetic variation and *de-novo* mutations. The black line corresponds to eq. (19), with the genetic background variation σ_g^2 determined by the SHC approximation (eq. 16). The grey curve gives the analytical prediction for substitutions from *de-novo* mutations under the assumption that the phenotypic lag δ_{eq} has reached an equilibrium (eq. 23). The red line gives the analytical prediction for the first substitution from *de-novo* mutations under the adaptive-walk assumption that there is no genetic background variation (KOPP and HERMISSON 2009b, eq. 14). Note that, for some parameter combinations, the simulated distribution from standing variation deviates from eq. (19). In particular, for small v, it approaches the "neutral" prediction eq. (25, see Fig. 3 , and for large v, it may approach the distribution from new mutations, eq. (23), see Fig. 5. Fixed parameters: $\Theta = 2.5$, $N = 2500$, $\sigma_m^2 = 0.05$.

993
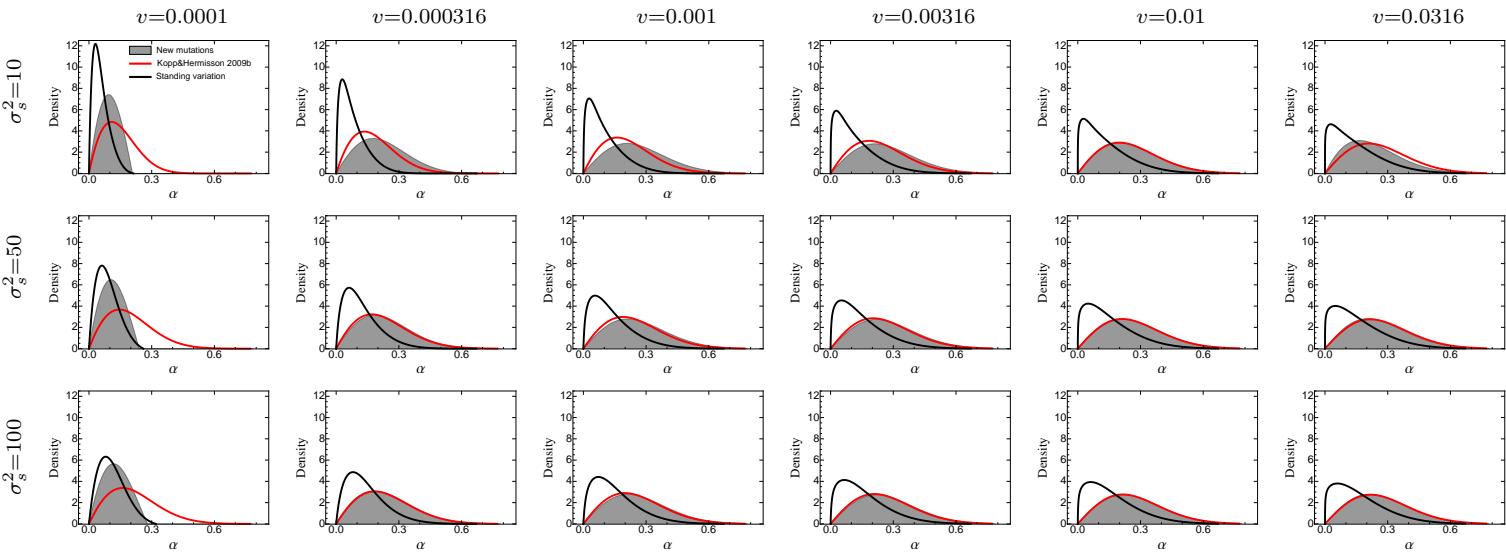
994

58

Figure S2__**2** – Comparison of the analytical predictions for the distribution of adaptive substitutions from standing genetic variation and *de-novo* mutations. For further details see Fig. S2__1. Fixed parameters: $\Theta = 5$, $N = 2500$, $\sigma_m^2 = 0.05$.
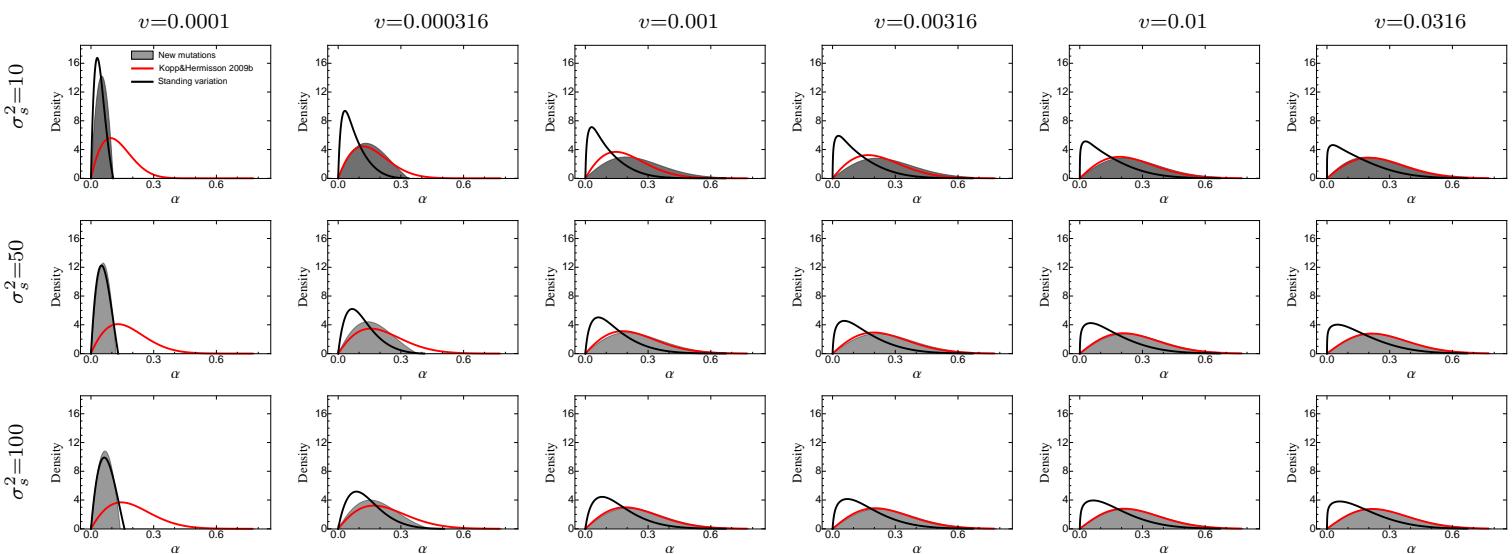
Figure S2__3 – Comparison of the analytical predictions for the distribution of adaptive substitutions from standing genetic variation and *de-novo* mutations. For further details see Fig. S2__1. Fixed parameters: $\Theta = 10$, $N = 2500$, $\sigma_m^2 = 0.05$.

997

998
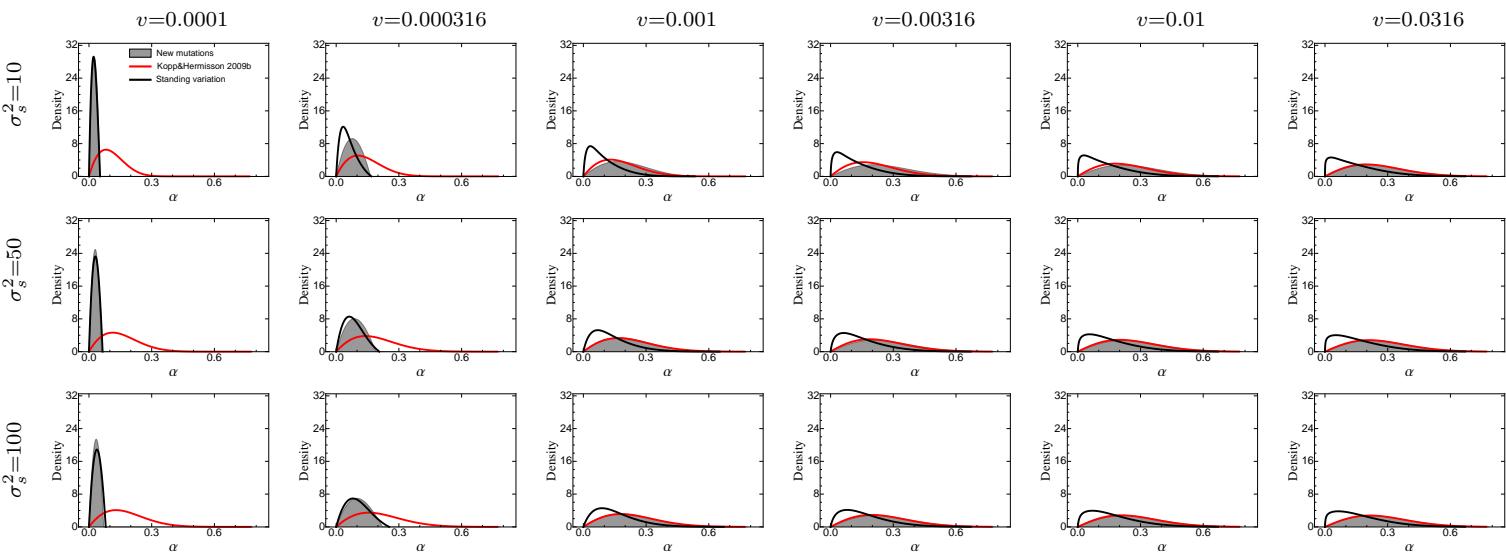
999 ## Supporting Information 3: Supporting Figures
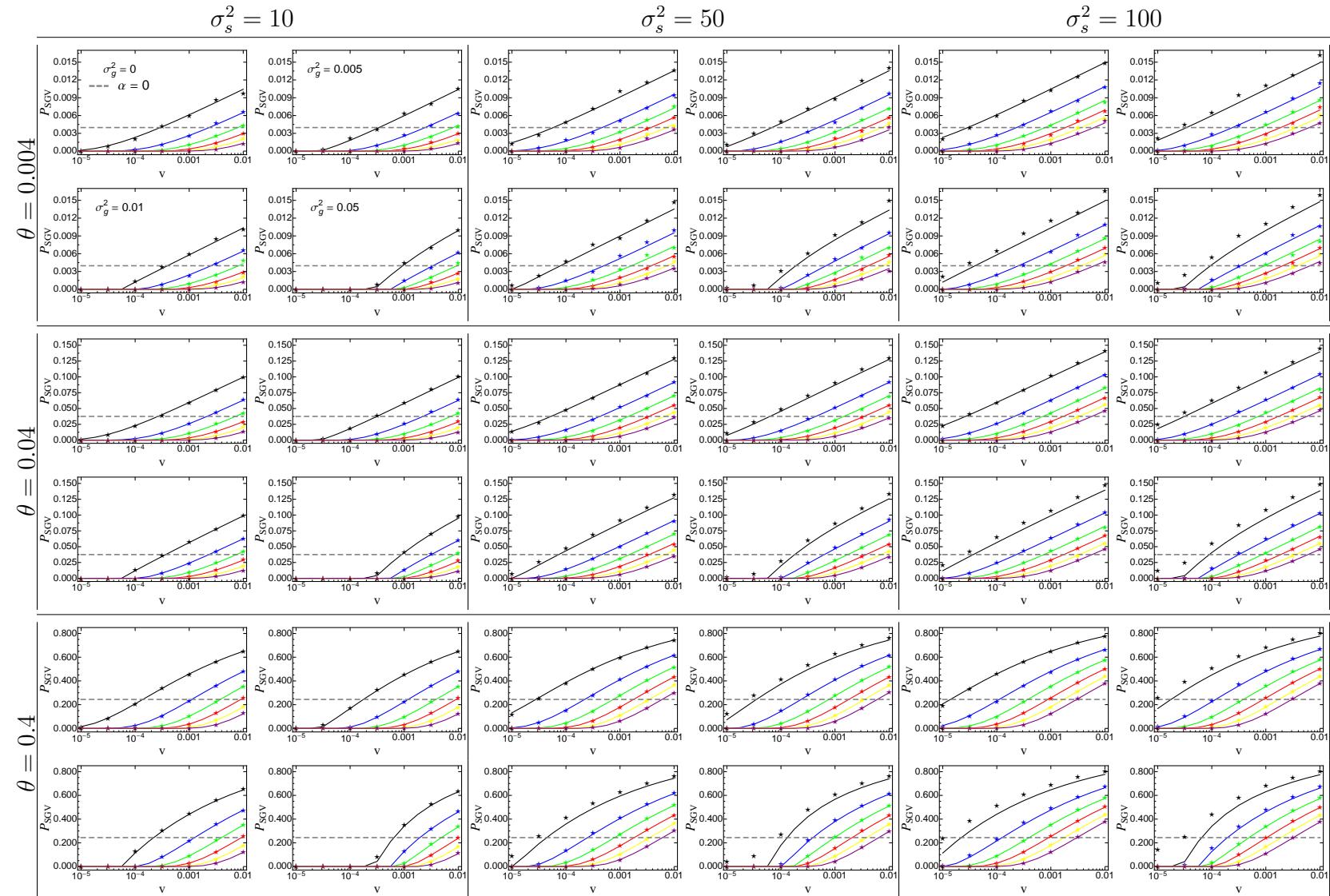
Figure S3_1 – The probability for a mutant allele to adapt from standing genetic variation as a function of the rate of environmental change v. Solid lines correspond to the analytical prediction (eq. 14), the grey dashed line shows the probability for a neutral allele ($\alpha = 0$; eq. 15), and symbols give results from Wright-Fisher simulations. The phenotypic effect size α of the mutant allele ranges from $0.5\sigma_m$ (top line; black) to $3\sigma_m$ (bottom line; purple) with increments of $0.5\sigma_m$. The figures in each parameter box (per locus mutation rate θ, width of fitness landscape σ_s^2) correspond to different values of the genetic background variation σ_g^2 with $\sigma_g^2 = 0$ (no background variation; top left), $\sigma_g^2 = 0.005$ (top right), $\sigma_g^2 = 0.01$ (bottom left) and $\sigma_g^2 = 0.05$ (bottom right). Other parameters: $N_e = 25000$, $\sigma_m^2 = 0.05$.

1000

1001

Figure S3_2 – The distribution of adaptive substitutions from standing genetic variation in the case of slow environmental change ($v = 10^{-5}$). Histograms show results from individual-based simulations. The blue line gives the analytical prediction (eq. 25), with σ_g^2 given by eq. 16), which assumes a neutral fixation probability. Fixed parameters: $\sigma_m^2 = 0.05$.
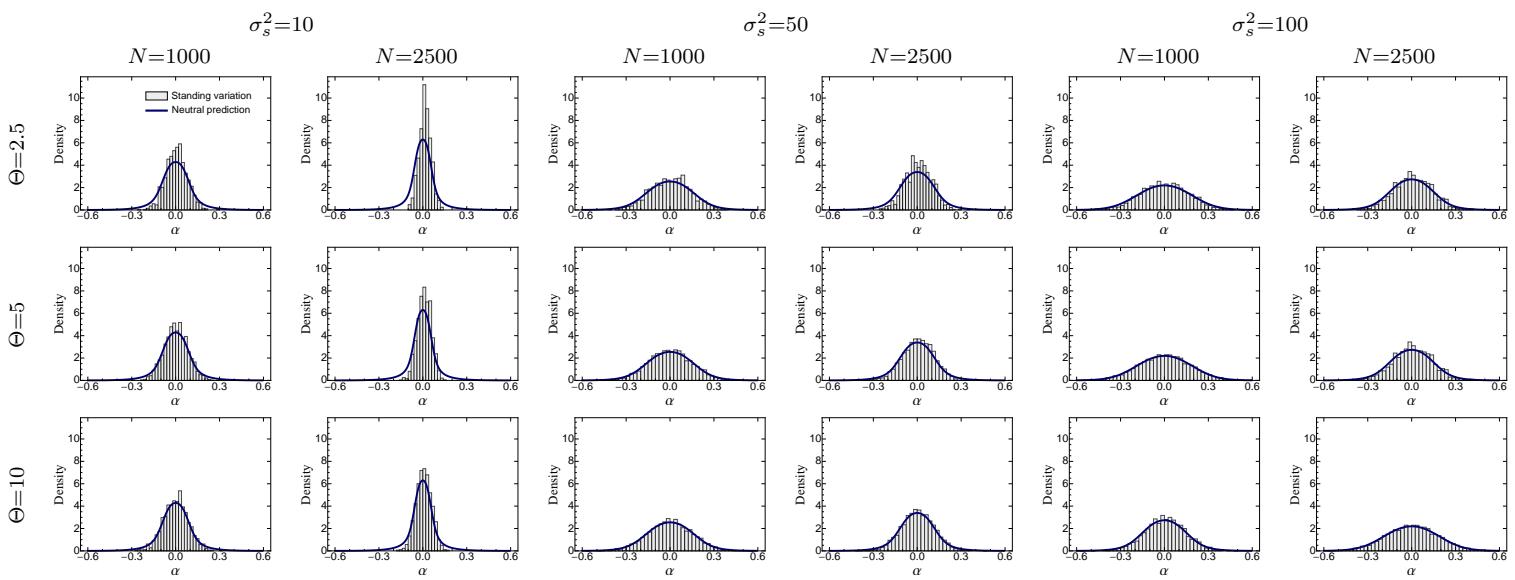
Figure S3_**3** – The average number of fixed adaptive substitutions from standing genetic variation, $|\mathcal{G}|_{\text{fix}}$, as a function of the rate of environmental change v, when standing genetic variation is the sole source for adaptation. Symbols show results from individual-based simulations (averaged over 100 replicate runs). The black line gives the analytical prediction (eq. 27) and the grey line corresponds to the average number of neutral fixations ($|\mathcal{G}|_{\text{fix},v\to0} = |\mathcal{G}| \int_{-\infty}^{\infty} p(\alpha)\Pi_{\text{seg},v\to0}(\alpha)\mathrm{d}\alpha$.). In both cases, σ_g^2 was taken from equation (16). Error bars for standard errors are contained within the symbols. Fixed parameters: $N = 1000$, $\sigma_m^2 = 0.05$.

1004

1005

64

Figure S3__4 – The average number of fixed adaptive substitutions from standing genetic variation, $|\mathcal{G}|_{\text{fix}}$, as a function of the rate of environmental change v, when standing genetic variation is the sole source for adaptation. Symbols show results from individual-based simulations (averaged over 100 replicate runs). The black line gives the analytical prediction (eq. 27) and the grey line corresponds to the average number of neutral fixations ($|\mathcal{G}|_{\text{fix},v\to 0} = |\mathcal{G}| \int_{-\infty}^{\infty} p(\alpha)\Pi_{\text{seg},v\to 0}(\alpha)\mathrm{d}\alpha$.). In both cases, σ_g^2 was taken from equation (16). Error bars for standard errors are contained within the symbols. Fixed parameters: $N = 2500$, $\sigma_m^2 = 0.05$.

1006

1007

65

Figure S3_**5** – The average number of fixed adaptive substitutions from standing genetic variation, $|\mathcal{G}|_{\text{fix}}$, as a function of the rate of environmental change v, when standing genetic variation is the sole source for adaptation. Symbols show results from individual-based simulations (averaged over 100 replicate runs). The black line gives the analytical prediction (eq. 27) and the grey line corresponds to the average number of neutral fixations ($|\mathcal{G}|_{\text{fix},v\to 0} = |\mathcal{G}| \int_{-\infty}^{\infty} p(\alpha)\Pi_{\text{seg},v\to 0}(\alpha)\mathrm{d}\alpha.$). In both cases, σ_g^2 was taken from equation (16). Error bars for standard errors are contained within the symbols. Fixed parameters: $N = 5000$, $\sigma_m^2 = 0.05$.

1008

1009

66

Figure S3**_6** – The average distance traversed in phenotype space, z^*, as a function of the rate of environmental change v, when standing genetic variation is the sole source for adaptation. Symbols show results from individual-based simulations (averaged over 100 replicate runs). The black line gives the analytical prediction (eq. 28), with σ_g^2 taken from equation (16). The grey-dashed line gives the critical rate of environmental change (eq. 29). Error bars for standard errors are contained within the symbols. Fixed parameters: $N = 1000$, $\sigma_m^2 = 0.05$.

1010

67
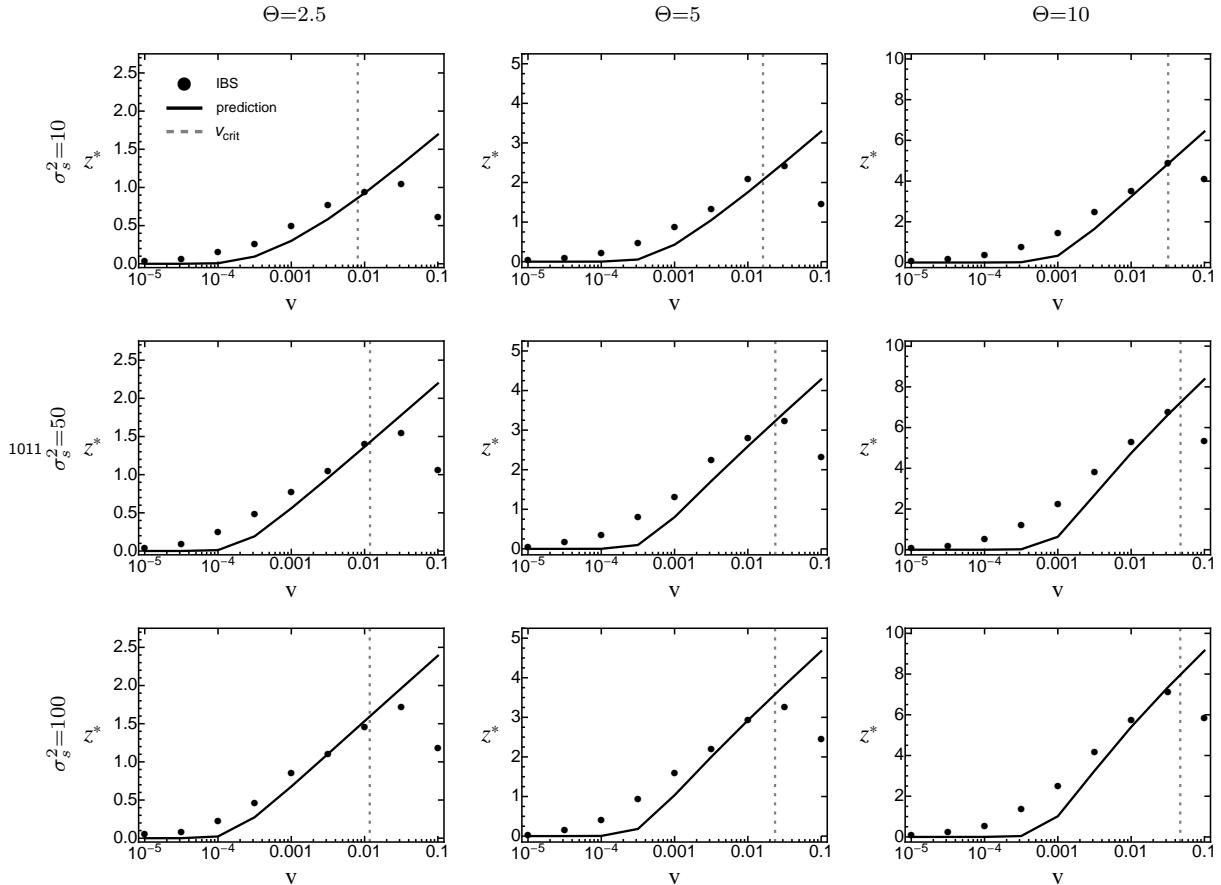
Figure S3__7 – The average distance traversed in phenotype space, z^*, as a function of the rate of environmental change v, when standing genetic variation is the sole source for adaptation. Symbols show results from individual-based simulations (averaged over 100 replicate runs). The black line gives the analytical prediction (eq. 28), with σ_g^2 taken from equation (16). The grey-dashed line gives the critical rate of environmental change (eq. 29). Error bars for standard errors are contained within the symbols. Fixed parameters: $N = 5000$, $\sigma_m^2 = 0.05$.

1012
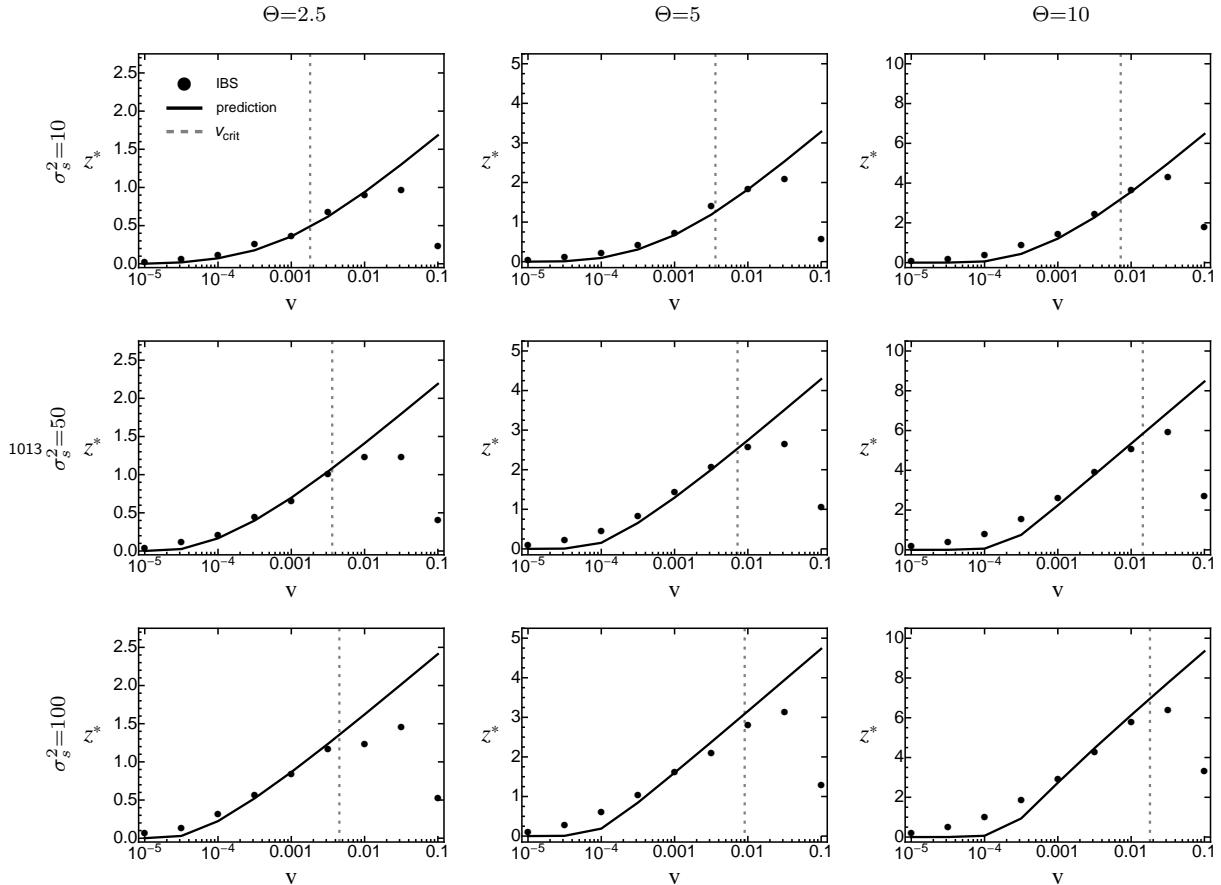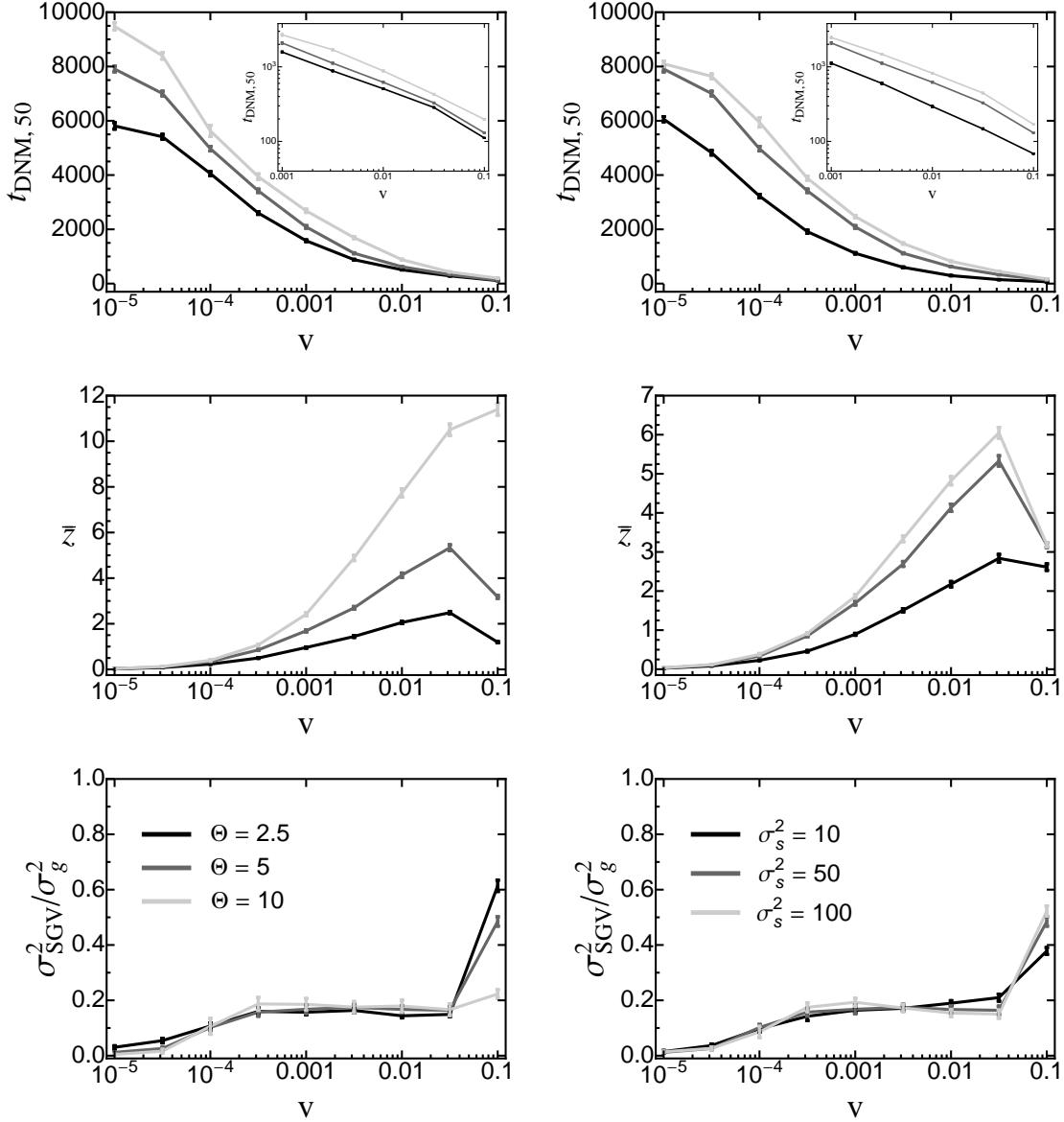
Figure S3__8 – First row: the point in time $t_{\mathrm{DNM},50}$ ($\bar{z}$) where 50% of the phenotypic response to moving-optimum selection have been contributed by *de-novo* mutations as a function of the rate of environmental change for various values of Θ (left) and σ_s^2 (right). Insets show the results for large v on a log-scale. Second row: The mean total phenotypic response at this time. Third row: The relative contribution of original standing genetic variation to the total genetic variance at time $t_{\mathrm{DNM},50}$ ($\bar{z}$). Data are means and standard errors from 1000 replicate simulation runs. Fixed parameters (if not stated otherwise): $\sigma_s^2 = 50$, $\Theta = 5$, $N = 1000$, $\sigma_m^2 = 0.05$.

Figure S3_9 – First row: the point in time $t_{\mathrm{DNM},50}\left(\sigma_g^2\right)$ where 50% of the genetic variance is composed of *de-novo* mutations as a function of the rate of environmental change for various values of Θ (left) and σ_s^2 (right). Insets show the results for large v on a log-scale. Second row: The mean total phenotypic response from standing genetic variation at this time. Third row: The relative contribution of original standing genetic variation to the total genetic variance at time $t_{\mathrm{DNM},50}\left(\sigma_g^2\right)$. Data are means and standard errors from 1000 replicate simulation runs. Fixed parameters (if not stated otherwise): $\sigma_s^2 = 50$, $\Theta = 5$, $N = 1000$, $\sigma_m^2 = 0.05$.

Figure S3_10 – First row: the point in time $t_{\mathrm{DNM},50}\left(\sigma_g^2\right)$ where 50% of the genetic variance is composed of *de-novo* mutations as a function of the rate of environmental change for various values of Θ (left) and σ_s^2 (right). Insets show the results for large v on a log-scale. Second row: The mean total phenotypic response from standing genetic variation at this time. Third row: The relative contribution of original standing genetic variation to the total genetic variance at time $t_{\mathrm{DNM},50}\left(\sigma_g^2\right)$. Data are means and standard errors from 1000 replicate simulation runs. Fixed parameters (if not stated otherwise): $\sigma_s^2 = 50$, $\Theta = 5$, $N = 2500$, $\sigma_m^2 = 0.05$.